frontiers in Marine Science

ORIGINAL RESEARCH
published: 10 September 2019
doi: 10.3389/fmars.2019.00522

Kinetic and Metabolic Isotope Effects in Zooxanthellate and Non-zooxanthellate Mediterranean Corals Along a Wide Latitudinal Gradient

Fiorella Prada[1†], Ruth Yam[2], Oren Levy[3], Erik Caroselli[1], Giuseppe Falini[4], Zvy Dubinsky[3], Stefano Goffredo[1] and Aldo Shemesh[2*†]*

[1] Marine Science Group, Department of Biological, Geological and Environmental Sciences, University of Bologna, Bologna, Italy, [2] Department of Earth and Planetary Sciences, Weizmann Institute of Science, Rehovot, Israel, [3] The Mina and Everard Goodman Faculty of Life Sciences, Bar–Ilan University, Ramat Gan, Israel, [4] Department of Chemistry "Giacomo Ciamician", University of Bologna, Bologna, Italy

OPEN ACCESS

Edited by:
Benoit Thibodeau, The University of Hong Kong, Hong Kong

Reviewed by:
Verena Schoepf, The University of Western Australia, Australia
Matthias López Correa, National Research Council, Italy

***Correspondence:**
Stefano Goffredo
s.goffredo@unibo.it
Aldo Shemesh
Aldo.Shemesh@weizmann.ac.il

† These authors have contributed equally to this work

Specialty section:
This article was submitted to Marine Biogeochemistry, a section of the journal Frontiers in Marine Science

Received: *26 March 2019*
Accepted: *12 August 2019*
Published: *10 September 2019*

Citation:
Prada F, Yam R, Levy O, Caroselli E, Falini G, Dubinsky Z, Goffredo S and Shemesh A (2019) Kinetic and Metabolic Isotope Effects in Zooxanthellate and Non-zooxanthellate Mediterranean Corals Along a Wide Latitudinal Gradient. Front. Mar. Sci. 6:522. doi: 10.3389/fmars.2019.00522

Many calcifying organisms exert significant biological control over the construction and composition of biominerals which are thus generally depleted in oxygen-18 and carbon-13 relative to the isotopic ratios of abiogenic aragonite. The skeletal $\delta^{18}O$ and $\delta^{13}C$ values of specimens of Mediterranean zooxanthellate (*Balanophyllia europaea* and *Cladocora caespitosa*) and non-zooxanthellate corals (*Leptopsammia pruvoti* and *Caryophyllia inornata*) were assessed along an 8° latitudinal gradient along Western Italian coasts, spanning ∼2°C and ∼37 W m^{-2} of annual average sea surface temperature and solar radiation (surface values), respectively. Seawater $\delta^{18}O$ and $\delta^{13}C_{DIC}$ were surprisingly constant along the ∼850 km latitudinal gradient while a ∼2 and ∼4% variation in skeletal $\delta^{18}O$ and a ∼4 and ∼9% variation in skeletal $\delta^{13}C$ was found in the zooxanthellate and non-zooxanthellate species, respectively. Albeit Mediterranean corals considered in this study are slow growing, only a limited number of non-zooxanthellate specimens exhibited skeletal $\delta^{18}O$ equilibrium values while all $\delta^{13}C$ values in the four species were depleted in comparison to the estimated isotopic equilibrium with ambient seawater, suggesting that these temperate corals cannot be used for thermometry-based seawater reconstruction. Calcification rate, linear extension rate, and skeletal density were unrelated to isotopic compositions. The fact that skeletal $\delta^{18}O$ and $\delta^{13}C$ of zooxanthellate corals were confined to a narrower range at the most isotopically depleted end compared to non-zooxanthellate corals, suggests that the photosynthetic activity may restrict corals to a limited range of isotopic composition, away from isotopic equilibrium for both isotopes. Our data show that individual corals within the same species express the full range of isotope fractionation. These results suggest that metabolic and/or kinetic effects may act as controlling factors of isotope variability of skeleton composition along the transect, and that precipitation of coral skeletal aragonite occurs under controlling kinetic biological processes, rather than thermodynamic control, by yet unidentified mechanisms.

Keywords: stable isotopes, vital effects, kinetic isotope effects, isotopic discrimination, Mediterranean Sea, temperate corals

INTRODUCTION

Scleractinian corals retain records of the chemical and physical conditions of the local surrounding seawater at the time of skeletal calcium carbonate accretion (McConnaughey, 2003; Allemand et al., 2004; Meibom et al., 2007), thus serving as oceanic recorders with monthly to seasonal resolution (McCulloch et al., 1999; Cohen et al., 2001; Felis et al., 2003). The skeletal carbon and oxygen isotopic ratios reflect temperatures, evaporation, precipitation, light intensity and primary production activity in the surrounding seawater but in a complex, and non-linear way (Levy et al., 2006; Rodrigues and Grottoli, 2006). In particular, skeletal $\delta^{18}O$ is the most commonly used proxy for seawater temperature and salinity (Al-Rousan et al., 2003; Asami et al., 2004; Linsley et al., 2006). In general, the isotopic composition of oceanic water masses changes as a result of water loss by evaporation, that enriches the heavy isotope species in the surface waters, and water inflow by precipitation and/or river discharge, which cause a decrease of $\delta^{18}O$ values of the oceanic water (Craig, 1961), thus revealing a direct relationship between salinity and $\delta^{18}O$ values. Moreover, at constant $\delta^{18}O$, an composition of seawater increase of 1°C in SST is coupled to a decrease in coral $\delta^{18}O$ of 0.18 to 0.22% (CorrelÌge, 2006). Coral skeletal $\delta^{18}O$ and $\delta^{13}C$ are generally shifted toward lower isotope values compared to aragonite in equilibrium with seawater (Weber and Woodhead, 1970, 1972; Weber, 1974; McConnaughey, 1989a). These so-called vital effects (Urey et al., 1951; Weber and Woodhead, 1972) or physiological effects (e.g., Epstein et al., 1951), may override environmental signals (e.g., Meibom et al., 2003, 2004; Rollion-Bard et al., 2003). However, in some cases, the environmentally controlled fraction that reflects the ambient temperature and isotopic composition of the water can be extracted and used for climatic reconstructions, as performed by Smith et al. (2000) in cold-water corals collected from the Norwegian Sea to the Antarctic.

Vital effects are the result of a biologically controlled calcification process (Wilbur and Simkiss, 1979; Allemand et al., 2004). In scleractinian corals, calcification is thought to occur within a physiologically controlled calcifying fluid (cf) in a semi-confined environment between the coral skeleton and its calicoblastic cell layer[8,9,10]. Carbonate chemistry of the calcifying fluid is exquisitely regulated through Ca^{2+}-ATPase proton pumps acting as Ca^{2+}/H^{+} exchangers (or antiporters), which remove two H^{+} ions from the calcifying fluid in exchange for every Ca^{2+} ion transported from the calicoblastic epithelial cells into the calcifying space (Al-Horani et al., 2003; Zoccola et al., 2004). By this process, calcifying fluid pH can be elevated significantly above ambient. Sources of dissolved inorganic carbon (DIC) can be either from seawater or from coral respiration and can be in the form of: (1) CO_2 freely diffusible across lipid membranes (Sueltemeyer and Rinast, 1996); and (2) bicarbonate (HCO_3^-) requiring specific carrier proteins (Furla et al., 2000; Vidal-Dupiol et al., 2013).

Physiological/vital effects can be attributed to "metabolic" or "kinetic" isotope fractionations. While metabolic effects are caused primarily by respiration and photosynthesis (Weber and Woodhead, 1970; Weber, 1974; Weber et al., 1976; Goreau, 1977a,b; Swart, 1983), kinetic effects associated with the hydration and hydroxylation of carbon dioxide during coral skeletogenesis result in simultaneous isotopic depletion of carbon and oxygen (relative to aragonite isotopic equilibrium; McConnaughey, 1989a,b). The prevailing hypothesis is that photosynthesis preferentially removes the light isotope of carbon from the internal pool of DIC while respiration enriches the pool in the light isotope (Weber and Woodhead, 1970; Weber, 1974; Weber et al., 1976; Goreau, 1977a,b; Swart, 1983). In general, since calcification in symbiotic corals should be on average three times higher during the day (Gattuso et al., 1999), when photosynthetic CO_2 uptake is several times faster than respiratory CO_2 release (McConnaughey, 1989a; McConnaughey et al., 1997), photosynthesis affects $\delta^{13}C$ up to 11% more strongly than respiration (about 1.5%). Thus, corals in which zooxanthellae are photosynthesizing rapidly will tend to show isotopically enriched skeletons compared to those in which photosynthesis is occurring much slower or does not occur at all (i.e., non-zooxanthellate species; Heikoop et al., 2000). Rollion-Bard et al. (2003) suggested that the observed $\delta^{18}O$ values reflect partial isotopic re-equilibration with water following kinetic CO_2 hydration/hydroxylation reactions while Adkins et al. (2003) proposed a quantitative (carbonate based) model to explain both carbon and oxygen fractionations. Both models allowed a "leak" of seawater to the calcifying sites. Recently, Chen et al. (2018) expanded this model and incorporated carbonic anhydrase activity to better explain the mechanism and the depletion relation between $\delta^{18}O$ and $\delta^{13}C$. It is widely recognized that vital effects are not always constant within a genus or species, or even within individual corals, with faster growing individuals or faster growing parts of coral skeletons being generally more depleted in both $\delta^{18}O$ and $\delta^{13}C$ (e.g., Land et al., 1975; McConnaughey, 1989a; Cohen and McConnaughey, 2003). In fact, it has been observed that biomineralization in corals does not follow classical thermodynamic rules but rather responds to biological kinetic effects, following a mechanism that has not yet been unraveled (Juillet-Leclerc et al., 2018). McConnaughey (1989a) investigated zooxanthellate and non-zooxanthellate coral species from the in an attempt to same growth environment unravel the chemical mechanisms behind vital effects. His results showed that the photosynthetic *Pavona* had higher $\delta^{13}C$ than the non-photosynthetic *Tubastrea*, suggesting that algal preferential uptake of ^{12}C leaves the residual inorganic calcification "pool" enriched in ^{13}C, thereby increasing the $\delta^{13}C$ of the skeleton. Moreover, McConnaughey (1989b) concluded that skeleton carbonate precipitation must be fast enough to allow absorption of HCO_3^- and/or CO_3^{2-}, formed by CO_2 hydration and hydroxylation, before they isotopically re-equilibrate with seawater.

In the Mediterranean Sea, coral-based paleoclimatic studies are limited compared to tropical regions. Temperate seas like the Mediterranean are characterized by pronounced seasonal irradiance, temperature, and nutrient cycles, while high temperature and irradiance, and low nutrients are far less variable in tropical seas (Ferrier-Pagès et al., 2012). The Mediterranean basin is considered an oligotrophic basin (Sournia, 1973), with generally low chlorophyll concentration, with the exception

of a large bloom observed in the Liguro-Provencal Region (D'Ortenzio and Ribera d'Alcalà, 2009). Along the western Italian coast, the wind effect, coastal upwelling, and winter layers mixing, determine a decrease in the biomass of phyto- and zooplankton from north to south (D'Ortenzio and Ribera d'Alcalà, 2009). Local currents and rock composition at the Genova site considered in this study generate particular local conditions leading to higher SSTs than expected at that latitude [annual SST of Ligurian Sea = 18°C and Genova–Portofino (GN) = 19°C]. Moreover, the Strait of Messina, where the Scilla site is located, lies at the center of the Mediterranean Sea and is characterized by strong currents, including upwelling of deeper water of Levantine intermediate water origin (Cortese and De Domenico, 1990), which are colder, more salty and nutrient-rich with respect to the Tyrrhenian Surface Waters (Atlantic Water origin). Such environmental differences must be cautiously taken into account when investigating and interpreting the skeletal isotope signal of temperate corals. Stable isotope and trace element composition, in combination with U-series and radiocarbon dating of the zooxanthellate coral *Cladocora caespitosa*, and of the cold-water corals *Desmophyllum dianthus*, *Lophelia pertusa*, and *Madrepora oculata* have been validated as high-resolution paleoenvironmental proxies (Peirano et al., 2004; Silenzi et al., 2005; Cohen et al., 2006; Montagna et al., 2008; López Correa et al., 2010; Trotter et al., 2011).

The aim of the present study was to investigate the species-specific variation of skeletal $\delta^{18}O$ and $\delta^{13}C$ and "vital effects" in four Mediterranean scleractinian species along an 8° latitudinal gradient along the Italian coast. We collected and analyzed the colonial zooxanthellate *C. caespitosa* (Linnaeus, 1767), the solitary zooxanthellate *Balanophyllia europaea* (Risso, 1826), and the two solitary non-zooxanthellates *Leptopsammia pruvoti* Lacaze-Duthiers, 1897 and *Caryophyllia inornata* (Duncan, 1878). We measured the surrounding seawater $\delta^{18}O$ and $\delta^{13}C$ of DIC to determine the fractionation between coral skeletons and seawater during calcification.

MATERIALS AND METHODS

Sample Collection and Treatment

Specimens of four coral species and seawater samples were collected between July 2010 and June 2013 from six sites along a wide latitudinal gradient spanning ∼850 km and ∼2°C of average sea surface temperature along the Western Italian coast (44°20′N to 36°45′N; **Figure 1** and **Table 1**). *B. europaea* and *C. caespitosa* specimens were randomly collected along a reef with southerly exposure at a depth of 5–7 m. All four coral species occur at all six sites, except for *C. caespitosa* which was not sampled at Scilla. *Leptopsammia pruvoti* and *C. inornata* specimens were randomly collected on the vault of crevices at a depth of 15–18 m, except for the Elba site where *C. inornata* was collected under the wings of a sunken plane wreck, at a depth of 12–15 m. Coral tissue was removed by immersing the samples in a solution of 10% commercial bleach for 3 days. Corals were dried for 4 days at a maximum temperature of 50°C to avoid phase transitions in the skeletal carbonate (Vongsavat et al., 2006). Samples were inspected under a binocular microscope to remove fragments of substratum and calcareous deposits produced by other organisms. Polyp length (L: maximum axis of the oral disc), width (W: minimum axis of the oral disc), and height (h: oral–aboral axis) were measured using a pair of calipers (cf. Goffredo et al., 2007) and dry skeletal mass was weighed using an analytical balance (±0.1 mg).

Seawater samples for $\delta^{18}O$ (N = 5–8 per site at 6 and 16 m depth; **Table 2**) were collected by SCUBA in 50 ml plastic bottles, sealed, and kept in a refrigerator at 4°C for 3–6 months prior to analysis. Seawater samples for $\delta^{13}C$ of dissolved inorganic carbon (DIC; N = 2–5 per site at 6 and 16 m depth; **Table 2**) were collected by SCUBA in borosilicate-glass bottles, and 1 ml of saturated mercuric chloride ($HgCl_2$) was introduced to 100 ml of seawater in order to stop all biological activity. The bottles were kept in a refrigerator at 4°C for 3–6 months prior to analysis. Water samples were collected in duplicate.

Carbon and Oxygen Isotopic Compositions

For skeletal $\delta^{13}C$ and $\delta^{18}O$ analysis, the whole corallite, which represents approximately the past 5–20 years of growth, was ground in a mortar to obtain a fine and homogeneous powder. Skeletal $CaCO_3$ samples of 220–250 μg were reacted with 100% orthophosphoric acid and CO_2 gas was analyzed using a Finnigan GasBench II connected in line to a Finnigan MAT 252 isotope ratio mass spectrometer. Calibration was maintained by routine analyses of internal and international standards. The long-term precision of our internal laboratory standard is 0.06 and 0.10% for carbon and oxygen, respectively. Oxygen isotopes analysis of sea water ($\delta^{18}O_{sw}$) were carried out by equilibrating 0.5 ml of samples with a mixture of 0.5% CO_2 in He at 25°C for 24 h. The samples were analyzed on a Gas Bench II connected in line to a Finnigan MAT 252 mass spectrometer. The results are reported relative to the Vienna Standard Mean Ocean Water (VSMOW) with 0.05% (±1σ) long-term precision of laboratory working standard.

For seawater $\delta^{13}C$ of DIC ($\delta^{13}C_{DIC}$) analysis, 1 ml of seawater was injected into gas vials pre-flushed with He, then acidified with 0.15 ml H_3PO_4 and left to react for 24 h in 25°C. The samples were analyzed on a Gas Bench II and Finigan MAT 252. The results are reported relative to the international Vienna-PeeDee Belemnite (VPDB) standard with 0.08% long-term precision (±1σ) of $NaHCO_3$ laboratory standard (chemically pure). The coral $\delta^{13}C_{skeleton}$ and $\delta^{18}O_{skeleton}$ data are reported against VPDB-standard.

Growth Parameters

The mean annual calcification rate (mass of $CaCO_3$ deposited per year per area unit) was calculated for each specimen by applying the following formula: calcification (mg mm^{-2} yr^{-1}) = skeletal density (mg mm^{-3}) × linear extension (mm yr^{-1}) (Lough and Barnes, 2000; Carricart-Ganivet, 2004). Corallite length (L, maximum axis of the oral disc), width (W, minimum axis of the oral disc), and height (h, oral-aboral axis) were measured with calipers and the dry skeletal mass (M) was measured with a precision balance. Corallite volume was calculated using the

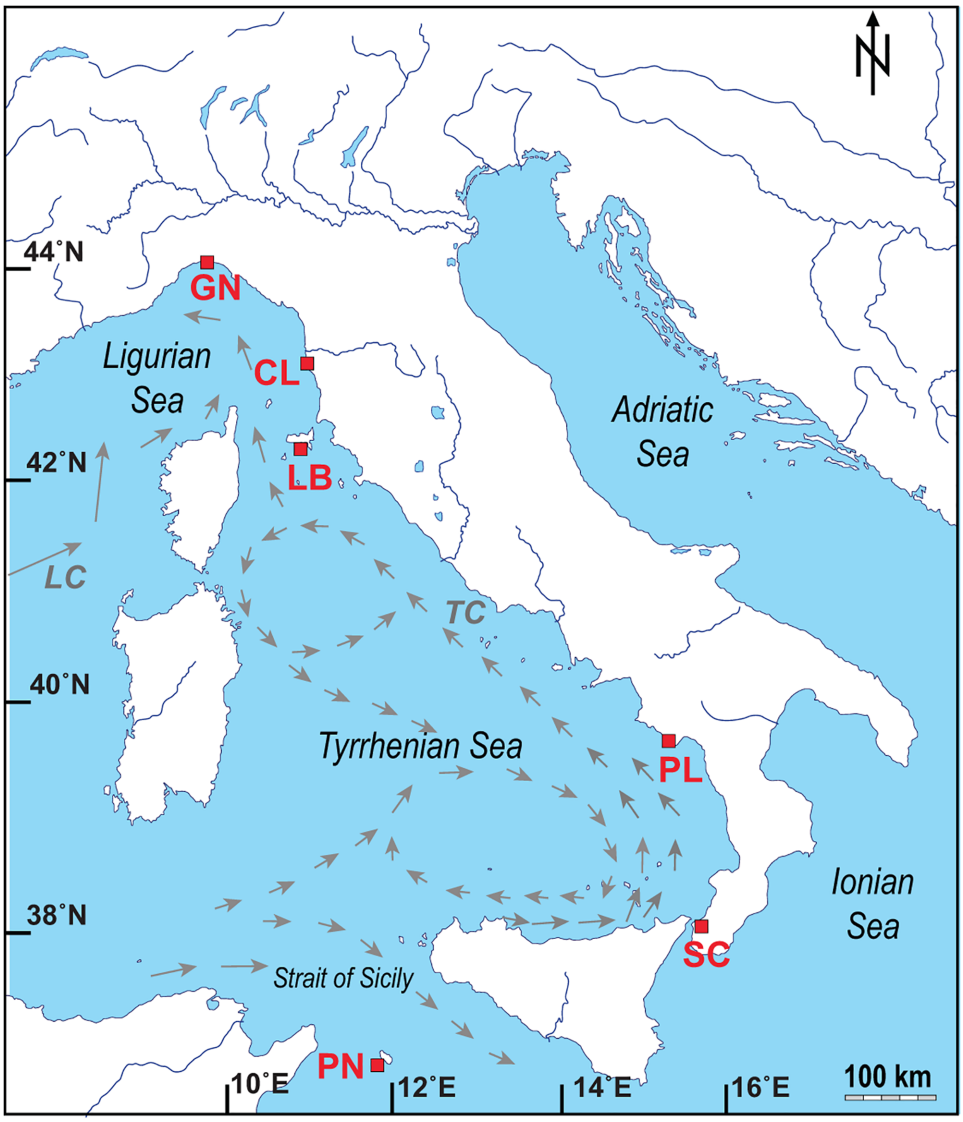

FIGURE 1 | Map of the Italian coastline indicating the sites where the corals and seawater samples were collected, with pattern of the main currents for the Ligurian Sea and Tyrrhenian Sea (modified from Silenzi et al., 2005; LC: Ligurian–Provencal Current; TC: Tyrrhenian Current). Abbreviations and coordinates of the site in decreasing order of latitude: GN Genova, 44°20′N, 9°08′E; CL Calafuria, 43°27′N, 10°21′E; LB Elba Isle, 42°45′N, 10°24′E; PL Palinuro, 40°02′N, 15°16′E; SC Scilla, 38°01′N, 15°38′E; PN Pantelleria Isle, 36°45′N, 11°57′E.

formula: $V = L^2 \times W^2 \times h\pi$ (Goffredo et al., 2007) The skeletal density for each corallite was calculated as M/V and the linear extension as L/age.

The age of each specimen was estimated by applying the Von Bertalanffy growth function, using the asymptotic length and growth constants for each population following Goffredo et al., 2008 for *B. europaea*, Caroselli et al., 2012b for *L. pruvoti*, and Caroselli et al., 2016b for *C. inornata*.

Environmental Parameters

Average monthly values of salinity were obtained using the Copernicus Marine Service Product MEDSEA_REANALYSIS_PHYS_006_004[1], and visualized through the Panoply software version 4.10.4[2]. Monthly at-depth temperatures (DT) at 6 m were obtained from Airi et al. (2014) and at 16 m were obtained from Caroselli et al. (2016a). Monthly values of solar radiation (SR; in W m^{-2}) were obtained from Caroselli et al. (2016a). Temperature data (°C) were recorded by digital thermometers (i-Button, DS1921G-F5#, Maxim Integrated Products, Dallas Semiconductors) placed at the sampling location (∼ 6 or 16 m depth, depending on the species) for each population. Sea Surface Temperature

[1]http://marine.copernicus.eu/

[2]http://www.giss.nasa.gov/tools/panoply/

TABLE 1 | Solar radiation (SR) values at sea surface and sampling depth temperature (DT) at 6 and 16 m at each site.

Site	Code	Latitude	SR (W m^{-2}), annual mean	DT (°C) at 6 m, annual mean	DT (°C) at 16 m, annual mean
Pantelleria	PN	36°45′N	212.3 (110.9–320.9)	19.81 (16.68–23.15)	19.15 (15.64–22.89)
Scilla	SC	38°01′N	203.2 (101.1–316.1)	18.63 (15.99–21.68)	18.21 (15.28–21.62)
Palinuro	PL	40°02′N	195.3 (88.5–310.1)	19.05 (15.29–23.40)	18.66 (15.33–22.52)
Elba	LB	42°45′N	184.2 (80.9–293.5)	18.09 (14.33–22.43)	17.64 (14.11–21.70)
Calafuria	CL	43°27′N	175.8 (73.6–283.5)	17.60 (13.43–21.72)	16.73 (13.09–20.34)
Genova	GN	44°20′N	162.0 (72.8–255.4)	18.95 (14.54–23.72)	18.35 (14.57–22.43)
Average				18.69 (15.04–22.68)	18.12 (14.67–21.92)

Values are averages of the 6 years preceding the sampling (n = 72). In brackets the average min (December, January, and February) and max (June, July, and August) values. The sites are arranged in increasing order of latitude. Solar radiation data from Caroselli et al. (2016b); temperature data for 6 m from Airi et al. (2014); temperature data for 16 m from Caroselli et al. (2016b).

TABLE 2 | Linear regression and correlation analysis between skeletal $\delta^{13}C$ and $\delta^{18}O$ in the four individual species and for each group, zooxanthellate and non-zooxanthellate species.

	Slope	SE	Intercept	SE	*n*	r^2	*r*
Balanophyllia europaea	0.43	0.05	−1.07	0.29	30	0.69	0.83**
Cladocora caespitosa	0.36	0.10	−0.36	0.51	25	0.37	0.61*
Leptopsammia pruvoti	0.33	0.03	1.30	0.11	30	0.84	0.92**
Caryophyllia inornata	0.31	0.02	−0.66	0.11	30	0.89	0.95**
All zoox species	0.40	0.05	−0.16	0.27	55	0.55	0.74**
All non-zoox species	0.34	0.02	1.10	0.10	60	0.83	0.91**

*r^2, Pearson's coefficient of determination; r, Pearson's correlation coefficient; SE, standard error; *p < 0.010, **p < 0.001. Zooxanthellate species (B. europaea and C. caespitosa); Non-zooxanthellate species (C. inornata and L. pruvoti).*

historical data (SST;°C) were obtained for each site from the National Mareographic Network of the Superior Institute for the Environmental Protection and Research (ISPRA[3]). Site-by-site, historical at-depth temperatures were estimated by linear regression produced between the temperature data recorded by the digital thermometers and SST. Monthly values of solar radiation (SR; W m^{-2}) were obtained from the databank of the Satellite Application Facility on Climate Monitoring (CM-SAF/EUMETSAT[4]) and represent values at sea surface. In this study, the average DT and SR of the 6 years preceding sampling (n = 72 monthly temperatures) was considered based on the mean turnover time of populations (calculated as the reciprocal of the instantaneous rate of mortality, Z; Caroselli et al., 2016a,b).

Statistical Analyses

One-way analysis of variance (ANOVA) was used to compare environmental parameters, seawater and coral isotope data among sites. Data were checked for normality using a Kolmogorov-Smirnov's test and for variance homoskedasticity using a Levene's test. When assumptions for parametric statistics were not fulfilled, the non-parametric Kruskal-Wallis equality-of-populations rank test was used, including the Monte Carlo correction for small sample size (Gabriel and Lachenbruch, 1969). The Monte Carlo correction solves problems in non-parametric tests for small samples, because it estimates the *p*-value by taking a random sample from the reference set and studies its permutations (Senchaudhuri et al., 1995). Pearson's correlation coefficients were calculated to test the relationship between environmental parameters and latitude, between skeletal $\delta^{13}C$ and $\delta^{18}O$ in the four individual species and for each group, zooxanthellate (*B. europaea* and *C. caespitosa*) and non-zooxanthellate (*C. inornata* and *L. pruvoti*) species, and between skeletal $\delta^{13}C$ and $\delta^{18}O$ and skeletal parameters (i.e., net calcification rate, linear extension rate, and skeletal density) in three species (*B. europaea*, *C. inornata*, and *L. pruvoti*). Spearman's rank correlation coefficient was used to calculate the significance of the correlations between coral $\delta^{13}C$ and $\delta^{18}O$ and latitude and seawater temperature. Spearman's rank correlation coefficient is an alternative to Pearson's correlation coefficient (Altman, 1991). It is useful for data that are non-normally distributed and do not meet the assumptions of Pearson's correlation coefficient (Potvin and Roff, 1993). Analysis of covariance (ANCOVA) was used to examine differences in $\delta^{13}C$ and $\delta^{18}O$ regression slopes between species. All analyses were computed using SPSS 20.0.

[3]http://isprambiente.gov.it

[4]http://www.cmsaf.eu

RESULTS

Solar Radiation, Seawater Temperature, $\delta^{13}C$, and $\delta^{18}O$

Average DT and solar radiation (SR) both varied among sites (DT at 6 m, Kruskal Wallis test, χ = 16.9, n = 6,

TABLE 3 | Seawater stable isotope data at 6 and 16 m depth in 6 sites along the west coast of Italy (~850 km transect).

Site	Site code	Salinity (%)	Depth (m)	Sampling date	$\delta^{13}C_{DIC}$	$\delta^{18}O_{sw}$
PANTELLERIA	PN	37.80	6	September 2010	1.05	0.45
PANTELLERIA	PN	37.80	6	September 2010	1.07	
PANTELLERIA	PN	37.75	6	May 2011	1.06	0.26
PANTELLERIA	PN	37.75	6	May 2011	1.10	
PANTELLERIA	PN	37.65	6	June 2013		0.73
PANTELLERIA	PN	37.65	6	June 2013		0.73
PANTELLERIA	PN	37.65	6	June 2013		0.80
PANTELLERIA	PN	37.80	16	September 2010	1.13	0.36
PANTELLERIA	PN	37.80	16	September 2010	1.07	0.45
PANTELLERIA	PN	37.75	16	May 2011	1.04	0.35
PANTELLERIA	PN	37.75	16	May 2011	1.07	0.36
PANTELLERIA	PN	37.65	16	June 2013		0.81
PANTELLERIA	PN	37.65	16	June 2013		0.89
PANTELLERIA	PN	37.65	16	June 2013		0.85
SCILLA	SC	38.85	6	July 2010	1.18	0.34
SCILLA	SC	38.85	6	July 2010	1.21	0.28
SCILLA	SC	38.85	6	July 2010	1.16	0.44
SCILLA	SC	38.70	6	May 2011	0.73	0.80
SCILLA	SC	38.70	6	May 2011	0.84	0.76
SCILLA	SC	38.70	6	May 2013		0.75
SCILLA	SC	38.70	6	May 2013		0.86
SCILLA	SC	38.70	6	May 2013		0.97
SCILLA	SC	38.85	16	July 2010	1.13	0.24
SCILLA	SC	38.85	16	July 2010	1.14	0.40
SCILLA	SC	38.85	16	July 2010	1.00	0.74
SCILLA	SC	38.70	16	May 2011	0.91	0.73
SCILLA	SC	38.70	16	May 2011		0.98
SCILLA	SC	38.70	16	May 2013		0.97
SCILLA	SC	38.70	16	May 2013		1.06
PALINURO	PL	37.95	6	June 2010	1.11	0.63
PALINURO	PL	37.95	6	June 2010	1.06	0.38
PALINURO	PL	37.95	6	May 2011	0.99	0.57
PALINURO	PL	37.95	6	May 2011	0.92	0.61
PALINURO	PL	37.95	6	May 2013		0.86
PALINURO	PL	37.95	6	May 2013		0.86
PALINURO	PL	37.95	6	May 2013		0.97
PALINURO	PL	37.95	6	May 2013		0.93
PALINURO	PL	37.95	16	June 2010	0.92	0.54
PALINURO	PL	37.95	16	June 2010	1.05	0.52
PALINURO	PL	37.95	16	May 2011	1.06	0.60
PALINURO	PL	37.95	16	May 2011	0.98	0.71
PALINURO	PL	37.95	16	May 2013		0.91
PALINURO	PL	37.95	16	May 2013		0.82
PALINURO	PL	37.95	16	May 2013		0.89
ELBA	LB	38.25	6	July 2011	1.12	0.45
ELBA	LB	38.25	6	July 2011	1.09	0.52
ELBA	LB	38.20	6	December 2011	1.10	0.36
ELBA	LB	38.20	6	December 2011	0.96	0.36
ELBA	LB	38.10	6	May 2013		0.86
ELBA	LB	38.10	6	May 2013		0.96
ELBA	LB	38.10	6	May 2013		0.93
ELBA	LB	38.25	16	July 2011	1.13	0.47
ELBA	LB	38.25	16	July 2011	1.04	0.45

(Continued)

TABLE 3 | Continued

Site	Site code	Salinity (%)	Depth (m)	Sampling date	$\delta^{13}C_{DIC}$	$\delta^{18}O_{sw}$
ELBA	LB	38.20	16	December 2011	0.97	0.37
ELBA	LB	38.20	16	December 2011	0.95	
ELBA	LB	38.10	16	May 2013		1.04
ELBA	LB	38.10	16	May 2013		1.06
ELBA	LB	38.10	16	May 2013		1.01
CALAFURIA	CL	38.10	6	March 2011	0.70	0.42
CALAFURIA	CL	38.10	6	March 2011	0.61	0.47
CALAFURIA	CL	38.10	6	March 2011	0.69	0.38
CALAFURIA	CL	38.10	6	April 2013		0.81
CALAFURIA	CL	38.10	6	April 2013		0.95
CALAFURIA	CL	38.15	6	June 2013		0.73
CALAFURIA	CL	38.15	6	June 2013		0.92
CALAFURIA	CL	38.10	16	March 2011	0.68	0.52
CALAFURIA	CL	38.10	16	March 2011	0.76	0.61
CALAFURIA	CL	38.10	16	April 2013		0.87
CALAFURIA	CL	38.10	16	April 2013		0.87
CALAFURIA	CL	38.15	16	June 2013		1.02
CALAFURIA	CL	38.15	16	June 2013		0.95
GENOVA	GN	38.10	6	April 2011	1.02	0.41
GENOVA	GN	38.10	6	April 2011	0.94	0.44
GENOVA	GN	38.10	16	April 2011	0.97	0.54
GENOVA	GN	38.10	16	April 2011	0.89	0.49
GENOVA	GN	38.15	6	June 2013		0.77
GENOVA	GN	38.15	6	June 2013		0.74
GENOVA	GN	38.15	6	June 2013		0.73
GENOVA	GN	38.15	16	June 2013		0.96
GENOVA	GN	38.15	16	June 2013		0.78
GENOVA	GN	38.15	16	June 2013		0.74

$p < 0.010$; DT at 16 m, Kruskal Wallis test, $\chi = 21.7$, $n = 6$, $p < 0.010$; SR, Kruskal Wallis test, $\chi = 18.4$, $n = 6$, $p < 0.010$). While SR was negatively correlated with latitude (Pearson's correlation, $n = 6$, $p < 0.010$; **Figure 2A**), DT was not correlated with latitude (Pearson's correlation, $n = 6$, $p > 0.050$; **Figure 2B**). The 6 years average monthly values of SR ranged from 162.0 W m^{-2} at GN to 212.3 W m^{-2} at PN (**Table 1** and **Supplementary Table S1**). The 6 years average monthly seawater temperature exhibited an annual cycle in all sites, reaching summer maxima of 21.7–23.7°C and 20.3–22.9°C at 6 and 16 m depth, respectively, and winter minima of 13.4–16.7°C and 13.1–15.6°C at 6 and 16 m depth, respectively (**Table 1** and **Supplementary Tables S2**, **S3**). The temperature difference between 6 and 16 m depth was not significantly different (average temperature, *t*-Test, $t = 1.208$, $n = 12$, $p > 0.050$; average minimum temperature, *t*-Test, $t = 0.604$, $n = 12$, $p > 0.050$; average maximum temperature, *t*-Test, $t = 1.489$, $n = 12$, $p > 0.050$; **Supplementary Tables S2**, **S3**), in the order of 0.4–0.8°C for annual average and both, summer and winter months. The annual amplitude was maximal in Genova (∼8–9°C), and minimal in Scilla (∼6°C: **Supplementary Tables S2**, **S3**).

Average annual $\delta^{18}O_{sw}$ along the Italian western coast was 0.65 ± 0.23% (mean ± SD) at 6 m and 0.71 ± 0.24% at 16 m and ranged between 0.60 and 0.72% at 6 m and between 0.58 and 0.81% at 16 m depth. The average annual $\delta^{13}C_{DIC}$ along the transect was 0.99 ± 0.17% at 6 m and 0.99 ± 0.12% at 16 m relative to VPDB and ranged between 0.67 and 1.07% at 6 m and between 0.72 and 1.08% at 16 m depth. No significant differences in average annual $\delta^{18}O_{sw}$ were found among sites (Kruskal-Wallis test, $\chi = 1.611$, $\chi = 3.853$, $n = 40$ and $n = 38$ at 6 and 16 m depth, respectively, $p > 0.050$; **Figure 2C** and **Table 2**) which was remarkably constant along the 850 km North-South transect. Also, average annual $\delta^{13}C_{DIC}$ did not exhibit significant differences among sites either (Kruskal-Wallis test, $\chi = 9.232$, $\chi = 9.357$, $n = 22$ and $n = 20$ at 6 and 16 m depth, respectively, $p > 0.050$; **Figure 2D** and **Table 2**).

The isotopic value for a biological aragonite precipitated in quasi-equilibrium with ambient seawater along the latitudinal gradient, calculated from Grossman and Ku (1986) for oxygen [$T = 20.6 - 4.34(\delta^{18}O_{arag} - \delta^{18}O_{seawater}]$ and Romanek et al. (1992) for carbon ($\delta^{13}C_{arag} = \delta^{13}C_{DIC} + 2.7$), using the annual average temperature from all stations at both depths, resulted in 0.51% for $\delta^{18}O$ and 2.7% for $\delta^{13}C$ (**Figure 3**). Average $\delta^{18}O_{seawater}$ and $\delta^{13}C_{DIC}$ were not included in the equation as the graph axis is respectively, $\delta^{18}O_{arag} - \delta^{18}O_{seawater}$ and $\delta^{13}C_{arag} - \delta^{13}C_{DIC}$.

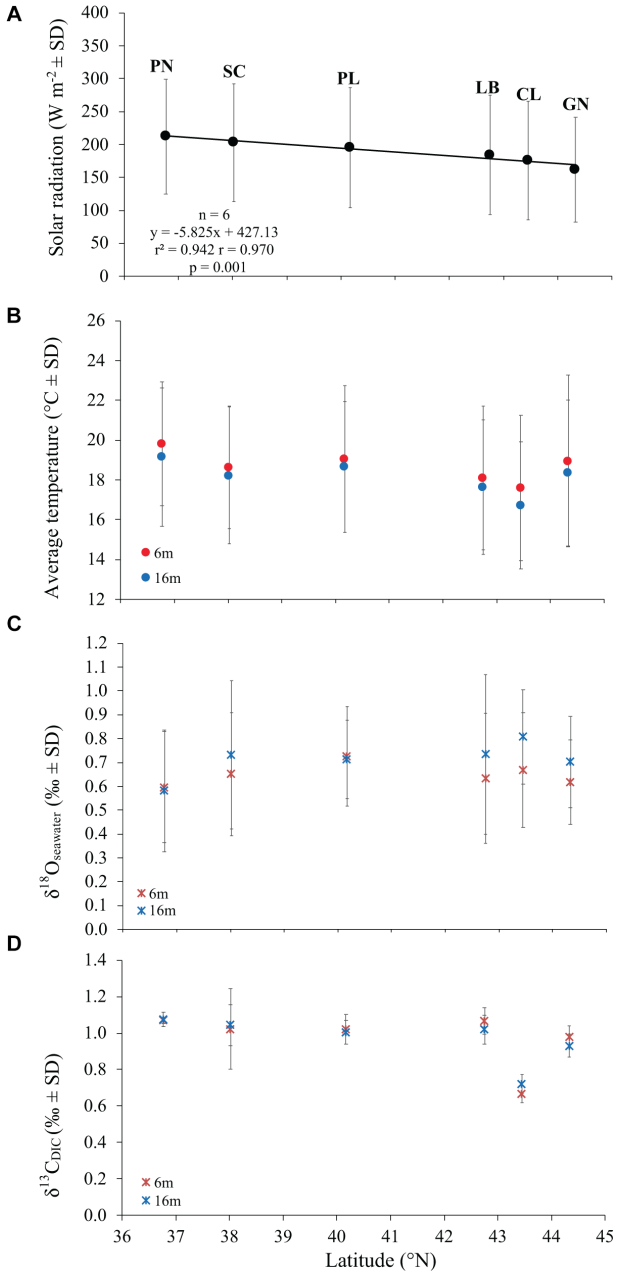

FIGURE 2 | The relation between average solar radiation values at sea surface **(A)**, temperature **(B)**, $\delta^{18}O_{seawater}$ **(C)**, and $\delta^{13}C_{DIC}$ **(D)** with latitude at 6 and 16 m depth in 6 sites along the west coast of Italy (~850 km transect).

Skeletal $\delta^{13}C$ and $\delta^{18}O$ and Growth Parameters

Average skeletal $\delta^{18}O$ and $\delta^{13}C$ along the gradient was −4.32 ± 0.71% (mean ± SD) and −1.66 ± 0.36%, respectively, in *B. europaea*, −4.28 ± 0.28% and −1.59 ± 0.19%, respectively, in *C. caespitosa*, −2.50 ± 1.21% and 0.88 ± 0.50%, respectively, in *L. pruvoti*, and −3.83 ± 1.14% and −0.09 ± 0.47%, respectively, in *C. inornata* (**Table 3**) relative to VPDB. Both skeletal $\delta^{13}C$ and $\delta^{18}O$ differed among sites in all species (*B. europaea,* ANOVA, $n = 30$, $p < 0.01$, $F = 4.904$ and $F = 5.240$, respectively; *C. caespitosa,* ANOVA, $n = 25$, $p < 0.001$, $F = 39.601$ and $F = 24.489$, respectively; *L. pruvoti,* ANOVA, $n = 30$, $p < 0.001$, $F = 13.212$ and $F = 8.049$, respectively; *C. inornata,* ANOVA, $n = 30$, $p < 0.001$, $F = 17.735$ and $F = 11.225$, respectively; **Table 3**). Skeletal isotope data are presented as $\delta^{13}C_{skeleton} - \delta^{13}C_{DIC}$ or $\delta^{18}O_{skeleton} - \delta^{18}O_{sw}$ in order to account for the isotopic composition of the local seawater in each site. A strong positive correlation between skeletal $\delta^{13}C$ and $\delta^{18}O$ was observed in all species (**Table 4**). The slopes within each group, zooxanthellate and non-zooxanthellate, did not differ (*B. europaea* vs *C. caespitosa*, ANCOVA, $F = 0.382$, $n = 30$ and 25, respectively; *L. pruvoti* vs *C. inornata,* ANCOVA, $F = 0.492$, $n = 30$ both species; $p > 0.050$; **Figure 3**). The slopes did not differ also between the two groups (zooxanthellate vs non-zooxanthellate, ANCOVA, $F = 0.994$, $n = 55$ and 60, respectively; $p > 0.050$; **Figure 3**). Latitude showed a significant positive correlation with both skeletal $\delta^{13}C$ and $\delta^{18}O$ in *B. europaea* (Spearman's correlation, $r^2 = 0.361$ and 0.438, respectively, $n = 30$, $p < 0.001$; **Figure 4**), and *C. caespitosa* (Spearman's correlation, $r^2 = 0.360$, $n = 25$, $p < 0.010$ and $r^2 = 0.214$, $n = 25$, $p < 0.050$, respectively; **Figure 4**). Solar radiation showed a symmetrical trend with a negative correlation with both skeletal $\delta^{13}C$ and $\delta^{18}O$ in *B. europaea* and *C. caespitosa* (**Supplementary Figure S1**). Generally, no significant correlation was found between skeletal $\delta^{18}O$ or $\delta^{13}C$ and average annual temperature, except for $\delta^{18}O$ of *C. inornata* which correlated positively (Spearman's correlation, $r^2 = 0.287$, $n = 30$, $p < 0.010$; **Supplementary Figure S2**). Skeletal $\delta^{13}C$ and $\delta^{18}O$ values of *B. europaea* were negatively correlated with average minimum temperature (Spearman's correlation, $r^2 = 0.301$, $n = 30$, $p < 0.001$ and $r^2 = 0.179$, $n = 30$, $p < 0.050$, respectively; **Figures 5A,B**), while skeletal $\delta^{18}O$ of *C. inornata* was positively correlated with average minimum temperature (Spearman's correlation, $r^2 = 0.201$; $n = 30$, $p < 0.050$; **Figure 5H**). Skeletal $\delta^{13}C$ and $\delta^{18}O$ values were positively correlated with average maximum temperature in *C. caespitosa* (Spearman's correlation, $r^2 = 0.232$, $n = 25$, $p < 0.050$ and $r^2 = 0.487$, $n = 25$, $p < 0.001$, respectively; **Figures 6C,D**) and *C. inornata* (Spearman's correlation, $r^2 = 0.182$, $n = 30$, $p < 0.050$ and $r^2 = 0.397$, $n = 30$, $p < 0.001$, respectively; **Figures 6G,H**).

Generally, no correlation was found between skeletal $\delta^{13}C$ and $\delta^{18}O$ and net calcification rate, linear extension rate, and skeletal density, in neither of the species, except for linear extension rate in *L. pruvoti* that showed a positive correlation with both $\delta^{13}C$ and $\delta^{18}O$ (Pearson's correlation, $r^2 = 0.288$, $n = 30$, $p < 0.010$ and $r^2 = 0.146$, $n = 30$, $p < 0.050$, respectively; **Figure 7** and **Table 3**).

DISCUSSION

This study investigated for the first time the skeletal $\delta^{18}O$ and $\delta^{13}C$ of individual specimens of zooxanthellate and non-zooxanthellate Mediterranean coral species and the stable isotope signature of the surrounding seawater collected along a ~850 km latitudinal gradient. Previous studies performed on the solitary zooxanthellate *B. europaea* along the same

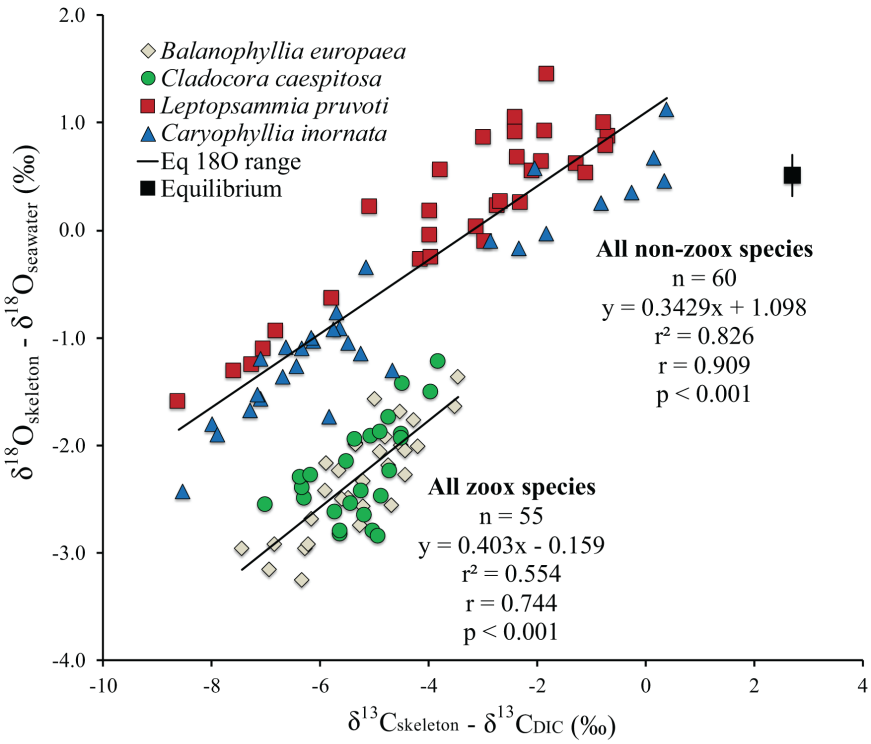

FIGURE 3 | Isotopic comparison between *Balanophyllia europaea* (zooxanthellate), *Cladocora caespitosa (*zooxanthellate), *Leptopsammia pruvoti* (non-zooxanthellate), and *Caryophyllia inornata* (non-zooxanthellate) at 6 sites along the west coast of Italy (∼850 km transect). Regression lines are the best fit to the zooxanthellate and non-zooxanthellate data sets. The black square indicates the estimated aragonite equilibrium value for average annual temperature for the 6 sites along the gradient using Grossman and Ku (1986) for oxygen and Romanek et al. (1992) for carbon. Vertical bar indicates equilibrium values corresponding to maximum and minimum average temperature. r^2, Pearson's coefficient of determination; *r*, Pearson's correlation coefficient; *n*, number of individuals.

latitudinal gradient considered in this study showed a reduction of the net calcification rate, which results in a progressive decrease of skeletal bulk density and an increase in skeletal porosity, especially of larger sized pores with increasing seawater temperature (Caroselli et al., 2011; Fantazzini et al., 2013). This determines a decrease of the resistance of the skeleton to mechanical stress (Goffredo et al., 2015). Furthermore, its population stability and abundance decrease with increasing temperature, as evidenced by a progressive lack of juveniles (Goffredo et al., 2007, 2008). On the other hand, the solitary non-zooxanthellate (i.e., asymbiotic) corals *L. pruvoti* and *C. inornata* appear insensitive to temperature along the same gradient (Goffredo et al., 2007, 2008, 2009; Caroselli et al., 2011, 2012a,b; Fantazzini et al., 2013). A study conducted along a natural temperature gradient in the Eastern Adriatic Sea on the colonial zooxanthellate coral *C. caespitosa* showed increases in net calcification rate with SST (Kružić et al., 2012), in contrast with laboratory observations showing that long-term exposure to high temperature led to a decrease in net calcification (Rodolfo-Metalpa et al., 2006). However, none of these studies investigated the species-specific variation of skeletal $\delta^{18}O$ and $\delta^{13}C$ under different temperature conditions.

In this study, a wide variation in both skeletal $\delta^{18}O$ and $\delta^{13}C$ (∼2 to ∼4% and ∼4 to ∼9%, respectively) was found among the investigated species which could be attributed to metabolic/kinetic effects, given the relatively limited seawater temperature difference (∼2°C annual average SST, which however, was not correlated with latitude) and the homogeneity of the seawater $\delta^{18}O$ and $\delta^{13}C_{DIC}$ measured along the gradient. Seawater $\delta^{18}O$ was remarkably constant along the 850 km transect with a restricted variation in salinity from 37.7 psu in Pantelleria to 38.1 psu in Genova, indicating that evaporation and precipitation and/or river discharges do not vary substantially along the gradient. Average $\delta^{18}O_{sw}$ values along our gradient (0.65 ± 0.23%) were lower than those measured for surface waters in the Eastern Mediterranean Sea by Pierre et al. (1986) (1.68%) and by Gat et al. (1996) (∼1.38%), probably as a result of higher temperature and salinity values compared to the Western Mediterranean Sea (Sakalli, 2017). Pantelleria seems to show slightly lower $\delta^{18}O_{sw}$ values along the latitudinal gradient, perhaps as a remnant of Atlantic water surface inflow, prior to increased evaporation, when moving north as Tyrrhenian Current (Paul et al., 2001). We also observed the lower $\delta^{18}O_{sw}$ values for the shallower sampling depths of 6 m in Elba, Calafuria and Genova, which could be linked to river inflow and salinity, however, we exclude this possibility as the average salinity would have to be lower than in the other locations, which is not the case. Further seawater isotope measurements are needed to verify

TABLE 4 | Coral aragonite stable isotope data and net calcification rate (mg mm^{-2} yr^{-1}), linear extension rate (mm yr^{-1}) and bulk skeletal density (mg mm^{-3}) in *Balanophyllia europaea*, *Leptopsammia pruvoti*, and *Caryophyllia inornata* at 6 sites along the west coast of Italy (~850 km transect).

Site	Site code	Species	Sample code	Sampling date	Depth (m)	$\delta^{13}C_{skeleton}$	$\delta^{18}O_{skeleton}$	Net calcification rate (mg mm^{-2} year^{-1})	Linear extension rate (mm year^{-1})	Skeletal density (mg mm^{-3})
PANTELLERIA	PN	*B. europaea*	BEU.PN.S10	8 September 2010	6	−5.78	−2.32	2.09	1.33	1.57
PANTELLERIA	PN	*B. europaea*	BEU.PNS16	8 September 2010	6	−6.36	−2.36	1.22	1.36	0.89
PANTELLERIA	PN	*B. europaea*	BEU.PN.S20	8 September 2010	6	−4.58	−1.64	1.21	1.26	0.96
PANTELLERIA	PN	*B. europaea*	BEU.PN.S33	8 September 2010	6	−4.53	−1.91	1.21	1.30	0.93
PANTELLERIA	PN	*B. europaea*	BEU.PN.S44	8 September 2010	6	−5.10	−2.09	1.92	1.39	1.38
PANTELLERIA	PN	*C. caespitosa*	CCA.PN.S01	10 September 2010	5	−4.54	−2.24			
PANTELLERIA	PN	*C. caespitosa*	CCA.PN.S02	10 September 2010	5	−4.34	−1.95			
PANTELLERIA	PN	*C. caespitosa*	CCA.PN.S03	10 September 2010	5	−4.10	−2.06			
PANTELLERIA	PN	*C. caespitosa*	CCA.PN.S04	10 September 2010	5	−4.54	−2.21			
PANTELLERIA	PN	*C. caespitosa*	CCA.PN.S05	10 September 2010	5	−4.65	−2.03			
PANTELLERIA	PN	*L. pruvoti*	PN.S13	8 September 2010	18	−2.88	0.32	0.93	0.72	1.29
PANTELLERIA	PN	*L. pruvoti*	PNS15	8 September 2010	18	−1.27	1.25	0.83	0.78	1.07
PANTELLERIA	PN	*L. pruvoti*	PN.S21	8 September 2010	18	−1.22	0.83	1.29	0.75	1.73
PANTELLERIA	PN	*L. pruvoti*	PN.S25	8 September 2010	18	−0.83	1.21	1.31	0.80	1.63
PANTELLERIA	PN	*L. pruvoti*	PN.S43	8 September 2010	18	−2.03	0.61	0.85	0.69	1.22
PANTELLERIA	PN	*C. inornata*	CIN.PN.S01	9 September 2010	17	−0.96	1.15	0.60	0.75	0.80
PANTELLERIA	PN	*C. inornata*	CIN.PN.S02	9 September 2010	17	1.45	1.70	0.52	0.74	0.71
PANTELLERIA	PN	*C. inornata*	CIN.PN.S03	9 September 2010	17	−4.67	−0.34	1.11	0.87	1.28
PANTELLERIA	PN	*C. inornata*	CIN.PN.S04	9 September 2010	17	−4.62	−0.19	1.01	0.81	1.25
PANTELLERIA	PN	*C. inornata*	CIN.PN.S05	9 September 2010	17	−4.07	0.24	0.50	0.73	0.68
SCILLA	SC	*B. europaea*	BEU.SC.S10	6 July 2010	6	−5.31	−2.60	1.45	1.19	1.22
SCILLA	SC	*B. europaea*	BEU.SC.S13	6 July 2010	6	−4.87	−1.51	0.87	0.99	0.87
SCILLA	SC	*B. europaea*	BEU.SC.S16	6 July 2010	6	−5.26	−2.31	1.32	1.28	1.03
SCILLA	SC	*B. europaea*	BEU.SC.S18	6 July 2010	6	−4.31	−1.33	0.76	1.08	0.70
SCILLA	SC	*B. europaea*	BEU.SC.S21	6 July 2010	6	−5.19	−2.27	1.15	1.36	0.85
SCILLA	SC	*L. pruvoti*	SC.S13	6 July 2010	18	−4.72	0.09	0.90	0.82	1.10
SCILLA	SC	*L. pruvoti*	SC.S17	6 July 2010	18	−6.19	−0.53	0.85	0.46	1.84
SCILLA	SC	*L. pruvoti*	SC.S18	6 July 2010	18	−5.75	−0.21	0.81	0.71	1.13
SCILLA	SC	*L. pruvoti*	SC.S19	6 July 2010	18	−7.56	−0.87	0.44	0.59	0.75
SCILLA	SC	*L. pruvoti*	SC.S35	6 July 2010	18	−6.54	−0.59	0.63	0.67	0.93
SCILLA	SC	*C. inornata*	CIN.SC.S03	6 July 2010	18	−6.93	−1.08	0.98	0.73	1.33
SCILLA	SC	*C. inornata*	CIN.SC.S10	6 July 2010	18	−6.04	−0.47	0.91	0.78	1.16
SCILLA	SC	*C. inornata*	CIN.SC.S12	6 July 2010	18	−6.84	−1.17	0.70	0.91	0.77
SCILLA	SC	*C. inornata*	CIN.SC.S22	6 July 2010	18	−7.48	−1.70	1.43	0.96	1.48
SCILLA	SC	*C. inornata*	CIN.SC.S36	6 July 2010	18	−6.23	−0.94	1.02	0.83	1.23

(Continued)

TABLE 4 | Continued

Site	Site code	Species	Sample code	Sampling date	Depth (m)	$\delta^{13}C_{skeleton}$	$\delta^{18}O_{skeleton}$	Net calcification rate (mg mm^{-2} year^{-1})	Linear extension rate (mm year^{-1})	Skeletal density (mg mm^{-3})
PALINURO	PL	*B. europaea*	BEU.PL.S05	1 July 2010	6	−3.41	−1.55	0.75	0.88	0.86
PALINURO	PL	*B. europaea*	BEU.PL.S11	1 July 2010	6	−4.19	−1.84	1.27	1.24	1.02
PALINURO	PL	*B. europaea*	BEU.PL.S12	1 July 2010	6	−3.49	−1.28	0.90	1.05	0.86
PALINURO	PL	*B. europaea*	BEU.PL.S17	1 July 2010	6	−3.42	−1.33	0.98	1.15	0.85
PALINURO	PL	*B. europaea*	BEU.PL.S35	1 July 2010	6	−4.25	−2.02	0.94	1.31	0.71
PALINURO	PL	*C. caespitosa*	CCA.PL.S01	1 July 2010	6	−4.47	−1.43			
PALINURO	PL	*C. caespitosa*	CCA.PL.S02	1 July 2010	6	−4.04	−1.20			
PALINURO	PL	*C. caespitosa*	CCA.PL.S03	1 July 2010	6	−3.71	−1.02			
PALINURO	PL	*C. caespitosa*	CCA.PL.S04	1 July 2010	6	−3.86	−1.16			
PALINURO	PL	*C. caespitosa*	CCA.PL.S05	1 July 2010	6–15	−4.32	−1.23			
PALINURO	PL	*L. pruvoti*	PL.S10	1 July 2010	16	−0.09	1.24	0.98	0.83	1.18
PALINURO	PL	*L. pruvoti*	PL.S11	1 July 2010	16	−1.66	0.98	1.28	0.80	1.60
PALINURO	PL	*L. pruvoti*	PL.S15	1 July 2010	16	−3.13	0.43	0.64	0.75	0.86
PALINURO	PL	*L. pruvoti*	PL.S34	1 July 2010	16	−1.07	1.26	0.67	0.78	0.86
PALINURO	PL	*L. pruvoti*	PL.S47	1 July 2010	16	0.25	1.71	0.78	0.85	0.92
PALINURO	PL	*C. inornata*	CIN.PL.A04	1 July 2010	14	0.18	0.96	0.79	0.80	0.99
PALINURO	PL	*C. inornata*	CIN.PL.A08	1 July 2010	14	1.16	1.39	0.62	0.79	0.79
PALINURO	PL	*C. inornata*	CIN.PL.B05	1 July 2010	14	0.75	1.06	0.75	0.80	0.94
PALINURO	PL	*C. inornata*	CIN.PL.B15	1 July 2010	14	1.36	1.17	0.82	0.90	0.91
PALINURO	PL	*C. inornata*	CIN.PL.F08	1 July 2010	14	−0.82	0.67	1.16	0.91	1.28
ELBA	LB	*B. europaea*	BEU.LB.S07	6 December 2010	6	−4.41	−1.85	2.50	1.62	1.54
ELBA	LB	*B. europaea*	BEU.LB.S24	6 December 2010	6	−3.62	−1.92	2.25	1.18	1.90
ELBA	LB	*B. europaea*	BEU.LB.S25	6 December 2010	6	−4.14	−1.70	1.78	1.18	1.52
ELBA	LB	*B. europaea*	BEU.LB.S35	6 December 2010	6	−5.86	−2.52	1.92	1.77	1.09
ELBA	LB	*B. europaea*	BEU.LB.S40	6 December 2010	6	−3.14	−1.37	2.78	1.45	1.91
ELBA	LB	*C. caespitosa*	CCA.LB.S01	6 December 2010	6	−5.21	−1.86			
ELBA	LB	*C. caespitosa*	CCA.LB.S02	6 December 2010	6	−5.26	−1.77			
ELBA	LB	*C. caespitosa*	CCA.LB.S03	6 December 2010	6	−5.93	−1.93			
ELBA	LB	*C. caespitosa*	CCA.LB.S04	6 December 2010	6	−5.29	−1.67			
ELBA	LB	*C. caespitosa*	CCA.LB.S05	6 December 2010	6	−5.08	−1.65			
ELBA	LB	*L. pruvoti*	LB.S01	7 December 2010	18	−4.05	0.94	0.81	0.73	1.11
ELBA	LB	*L. pruvoti*	LB.S04	7 December 2010	18	−0.79	2.18	0.62	0.62	0.98
ELBA	LB	*L. pruvoti*	LB.S12	7 December 2010	18	−1.70	0.95	0.53	0.66	0.80
ELBA	LB	*L. pruvoti*	LB.S26	7 December 2010	18	−1.37	1.64	0.64	0.70	0.92
ELBA	LB	*L. pruvoti*	LB.S27	7 December 2010	18	−2.76	1.29	0.65	0.76	0.85

(Continued)

TABLE 4 | Continued

Site	Site code	Species	Sample code	Sampling date	Depth (m)	$\delta^{13}C_{skeleton}$	$\delta^{18}O_{skeleton}$	Net calcification rate (mg mm^{-2} year^{-1})	Linear extension rate (mm year^{-1})	Skeletal density (mg mm^{-3})
ELBA	LB	*C. inornata*	CIN.LB.S07	6 December 2010	14	−5.10	−0.30	1.06	0.88	1.20
ELBA	LB	*C. inornata*	CIN.LB.S14	6 December 2010	14	−4.62	−0.18	0.52	0.74	0.70
ELBA	LB	*C. inornata*	CIN.LB.S18	6 December 2010	14	−6.07	−0.83	0.90	0.80	1.13
ELBA	LB	*C. inornata*	CIN.LB.S22	6 December 2010	14	−5.41	−0.53	0.73	0.99	0.74
ELBA	LB	*C. inornata*	CIN.LB.S35	6 December 2010	14	−5.32	−0.37	0.65	0.92	0.71
CALAFURIA	CL	*B. europaea*	BEU.CL.S09	4 February 2011	6	−3.61	−1.10	1.97	1.41	1.40
CALAFURIA	CL	*B. europaea*	BEU.CL.S10	4 February 2011	6	−5.23	−1.76	1.48	1.80	0.82
CALAFURIA	CL	*B. europaea*	BEU.CL.S21	4 February 2011	6	−2.85	−0.97	1.46	1.61	0.91
CALAFURIA	CL	*B. europaea*	BEU.CL.S24	4 February 2011	6	−4.23	−1.39	1.88	1.57	1.20
CALAFURIA	CL	*B. europaea*	BEU.CL.S26	4 February 2011	6	−4.07	−1.52	2.26	1.71	1.32
CALAFURIA	CL	*C. caespitosa*	CCA.CL.S01	24 March 2011	9	−4.18	−1.82			
CALAFURIA	CL	*C. caespitosa*	CCA.CL.S02	24 March 2011	9	−4.34	−2.13			
CALAFURIA	CL	*C. caespitosa*	CCA.CL.S03	24 March 2011	9	−4.57	−1.76			
CALAFURIA	CL	*C. caespitosa*	CCA.CL.S04	24 March 2011	9	−4.04	−1.57			
CALAFURIA	CL	*C. caespitosa*	CCA.CL.S05	24 March 2011	9	−4.25	−2.18			
CALAFURIA	CL	*L. pruvoti*	CL.S09	4 February 2011	16	−1.13	1.73	1.20	0.80	1.50
CALAFURIA	CL	*L. pruvoti*	CL.S17	4 February 2011	16	0.04	1.68	0.84	0.85	0.98
CALAFURIA	CL	*L. pruvoti*	CL.S20	4 February 2011	16	0.00	1.58	0.67	0.78	0.86
CALAFURIA	CL	*L. pruvoti*	CL.S26	4 February 2011	16	−2.23	0.70	0.76	0.82	0.92
CALAFURIA	CL	*L. pruvoti*	CL.S29	4 February 2011	16	−0.54	1.42	0.90	0.84	1.07
CALAFURIA	CL	*C. inornata*	CIN.CL.A07	24 March 2011	18	−2.14	0.70	2.10	1.04	2.03
CALAFURIA	CL	*C. inornata*	CIN.CL.A08	24 March 2011	18	−4.52	−0.34	1.42	1.03	1.37
CALAFURIA	CL	*C. inornata*	CIN.CL.B11	24 March 2011	18	−1.61	0.64	1.70	1.05	1.62
CALAFURIA	CL	*C. inornata*	CIN.CL.D02	24 March 2011	18	−5.12	−0.93	1.10	1.04	1.06
CALAFURIA	CL	*C. inornata*	CIN.CL.H01	24 March 2011	18	−3.94	−0.49	1.82	1.03	1.77
GENOVA	GN	*B. europaea*	BEU.GN.S03	14 April 2011	6	−3.55	−1.07	1.21	1.30	0.93
GENOVA	GN	*B. europaea*	BEU.GN.S05	14 April 2011	6	−4.36	−1.37	1.49	1.45	1.03
GENOVA	GN	*B. europaea*	BEU.GN.S19	14 April 2011	6	−4.02	−0.95	1.31	1.54	0.85
GENOVA	GN	*B. europaea*	BEU.GN.S21	14 April 2011	6	−2.49	−0.75	1.29	1.21	1.07
GENOVA	GN	*B. europaea*	BEU.GN.S28	14 April 2011	6	−3.83	−1.30	1.32	1.38	0.96
GENOVA	GN	*C. caespitosa*	CCA.GN.S01	14 April 2011	6	−3.48	−0.81			
GENOVA	GN	*C. caespitosa*	CCA.GN.S02	14 April 2011	6	−2.82	−0.61			
GENOVA	GN	*C. caespitosa*	CCA.GN.S03	14 April 2011	6	−2.96	−0.89			
GENOVA	GN	*C. caespitosa*	CCA.GN.S04	14 April 2011	6	−3.51	−1.28			
GENOVA	GN	*C. caespitosa*	CCA.GN.S05	14 April 2011	6	−3.50	−1.33			
GENOVA	GN	*L. pruvoti*	GN.S01	14 April 2011	16	−1.45	1.74	0.53	0.62	0.85

(Continued)

TABLE 4 | Continued

Site	Site code	Species	Sample code	Sampling date	Depth (m)	$\delta^{13}C_{skeleton}$	$\delta^{18}O_{skeleton}$	Net calcification rate (mg mm^{-2} year^{-1})	Linear extension rate (mm year^{-1})	Skeletal density (mg mm^{-3})
GENOVA	GN	*L. pruvoti*	GN.S08	14 April 2011	16	−3.04	0.65	0.66	0.68	0.97
GENOVA	GN	*L. pruvoti*	GN.S13	14 April 2011	16	−3.03	0.87	0.49	0.72	0.69
GENOVA	GN	*L. pruvoti*	GN.S35	14 April 2011	16	−6.11	−0.40	0.66	0.77	0.85
GENOVA	GN	*L. pruvoti*	GN.S49	14 April 2011	16	−2.03	1.56	0.66	0.72	0.91
GENOVA	GN	*C. inornata*	CIN.GN.A04	14 April 2011	15	−5.69	−0.39	0.62	0.85	0.73
GENOVA	GN	*C. inornata*	CIN.GN.A08	14 April 2011	15	−5.75	−0.66	0.61	0.89	0.69
GENOVA	GN	*C. inornata*	CIN.GN.A13	14 April 2011	15	−4.54	−0.35	0.67	0.98	0.68
GENOVA	GN	*C. inornata*	CIN.GN.E05	14 April 2011	15	−5.24	−0.30	1.10	0.94	1.17
GENOVA	GN	*C. inornata*	CIN.GN.F12	14 April 2011	15	−6.21	−0.83	0.76	0.94	0.80

whether this observation is maintained. The average annual $\delta^{13}C$ of the DIC also did not vary along the transect, suggesting that local primary production does not control the absolute value and is kept at the same level in coastal waters. Apparently, gas exchange and water mass characteristics override the primary production signal. The well mixed water column and the lack of stratified primary production is evident from the average annual $\delta^{13}C_{DIC}$ identity between 6 and 16 m.

At thermodynamic equilibrium, skeletal $\delta^{18}O$ is a function of temperature and $\delta^{18}O_{seawater}$ from which the coral deposited its $CaCO_3$. Hence, along the 850 km transect, where $\delta^{18}O_{seawater}$ shows small variations, changes in coral skeletal $\delta^{18}O$ should reflect changes in seawater temperature (Weber and Woodhead, 1972; Gagan et al., 2000; Kuhnert et al., 2000). The measured yearly average temperature change along the transect is about 2°C, yielding an expected skeletal $\delta^{18}O$ change of about 0.5% according to the coral aragonite temperature dependency (0.22% per 1°C; Epstein et al., 1953; Grossman and Ku, 1986; Böhm et al., 2000). Instead, a ∼2 and ∼4% variation in skeletal $\delta^{18}O$ was observed in the zooxanthellate and non-zooxanthellate species, respectively (**Figure 3**). The skeletal $\delta^{13}C$, which is strongly influenced by photosynthesis (light) and feeding (which directly affects the respired $\delta^{13}C$; McConnaughey, 2003), exhibits also a wide range, ∼4% for zooxanthellate corals and ∼9% for the non-zooxanthellate corals. These ranges, as well as the significant correlations between $\delta^{18}O$ and $\delta^{13}C$ in all species, point either to the metabolic and/or kinetic effects as possible controlling factors of isotope variability of skeleton composition along the transect (McConnaughey, 1989a; Smith et al., 2000; Schoepf et al., 2014). Given the difficulty in distinguish between kinetic and metabolic isotope effects, we applied the correction for kinetic isotope effects for $\delta^{13}C$ proposed by Heikoop et al., 2000, which however, did not improve the statistics or the interpretation of the data (**Supplementary Figure S3**) so we assume this correction does not work for our dataset. The full range of the isotope effect is presented in the $\delta^{18}O_{skeleton} - \delta^{18}O_{sw}$ vs $\delta^{13}C_{skeleton} - \delta^{13}C_{DIC}$ plot (**Figure 3**). The key observations from this plot are:

(1) The isotope range of non-zooxanthellate corals is much larger than that of the zooxanthellate corals in both carbon and oxygen.
(2) Each species encompasses the full range of its group, non-zooxanthellate or zooxanthellate.
(3) The regression lines are almost parallel within each group and did not differ between the two groups (**Table 4**).
(4) No corals exhibited equilibrium values as calculated for biogenic aragonite.
(5) The isotope range of different specimens on the 850 km transect is almost the same as that observed on a high resolution 2500 μm scale of the cold-water coral *D. cristagalli* from the Chilean Fjord (Adkins et al., 2003) and on a 4000 μm scale of the cold-water coral *L. pertusa* from Santa Maria di Leuca (Ionian Sea, Southern Italy; by López Correa et al., 2010). It is also comparable to the SIMS microanalysis $\delta^{18}O_{skeleton}$ range (Juillet-Leclerc et al., 2018) and the high-density bands

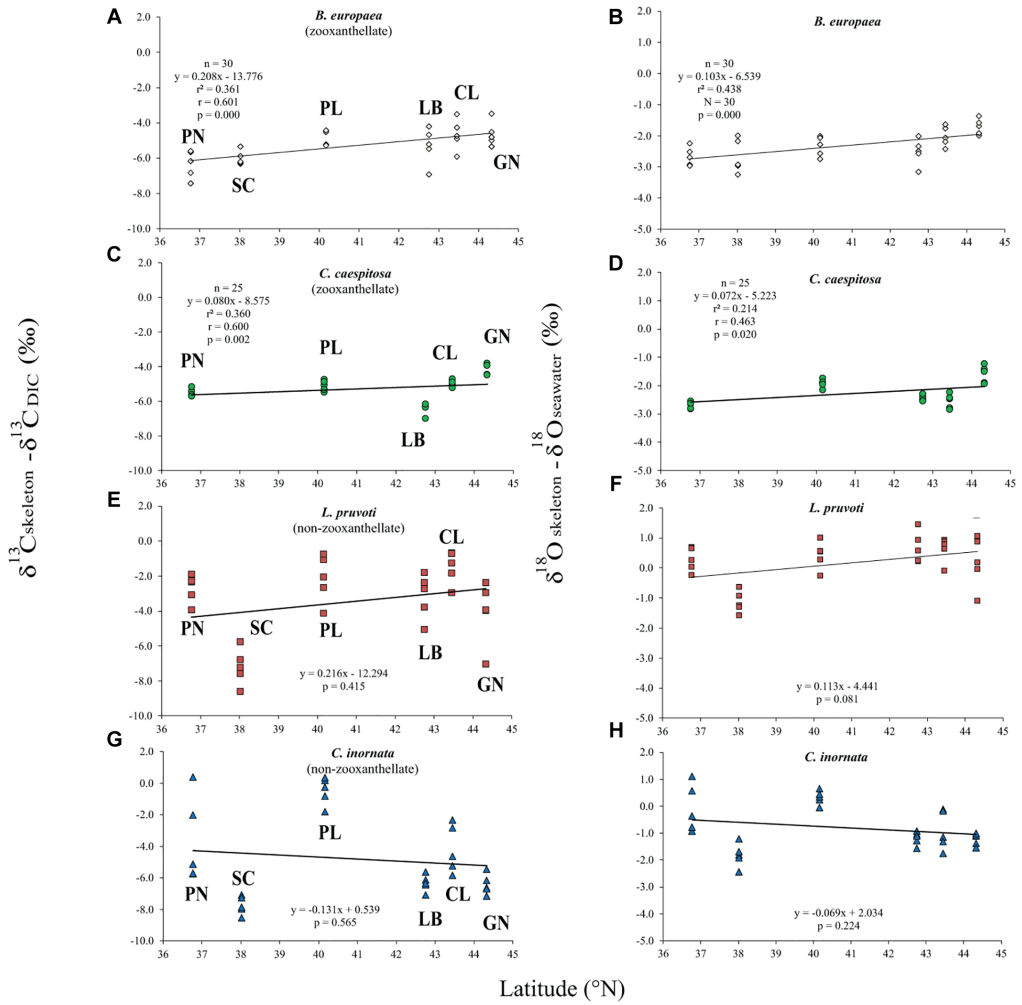

FIGURE 4 | The relation between skeletal $\delta^{13}C$ and $\delta^{18}O$ with latitude in *B. europaea* **(A,B)**, *C. caespitosa* **(C,D)**, *L. pruvoti* **(E,F)**, and *C. inornata* **(G,H)**. r^2, Spearman's determination coefficient; *r*, Spearman's correlation coefficient; *n*, number of individuals.

of *C. caespitosa* from a hundred year record in northwestern Mediterranean (Silenzi et al., 2005). Bulk analyses on mm scale resolution also exhibit a similar range for *Tubastrea* and *Pavona clavus* from the Galapagos (McConnaughey, 1989a).

Calcification rate, linear extension rate and skeletal density were suggested as factors which impact the isotopic composition of calcareous organisms such as corals (Land et al., 1975; Erez, 1978; McConnaughey, 1989a). Our results show that there is no correlation between any of these parameters and the measured isotope composition (**Figure 7**). This conclusion holds at the species level, regardless of their trophic strategy (i.e., non-zooxanthellate or zooxanthellate), all species being slow growing corals (∼0.7 to ∼3 mm yr^{-1}; Peirano et al., 1999). This finding contrasts McConnaughey's (1989a) assumption that rapid skeletogenesis favors strong kinetic effects. However, we cannot exclude the possibility that this result could also be due to the uncertainty associated with the estimated calcification data (see section "Materials and Methods"). The two zooxanthellate corals, *B. europaea* and *C. caespitosa* show significant correlations of $\delta^{18}O$ and $\delta^{13}C$ with latitude (**Figure 4**) being depleted with decreasing latitude and thus increasing solar radiation (**Figure 2** and **Supplementary Figure S2**). Given that algal photosynthesis can be inhibited by excessive irradiance (Cullen and Neale, 1994; Caroselli et al., 2015; Iluz and Dubinsky, 2015), the depleted skeletal $\delta^{13}C$ could result from inhibited photosynthesis of the symbiotic zooxanthellae at certain times in summer. This is in agreement with previous studies performed on *B. europaea* along this gradient, which highlighted negative effects on growth, population dynamics, and reproductive parameters (Goffredo et al., 2007, 2008, 2009, 2015; Caroselli et al., 2011; Fantazzini et al., 2013). Moreover, photosynthesis of zooxanthellae has temperature optima (Al-Horani, 2005), thus the decrease in $\delta^{13}C$ with increasing minimum temperature in *B. europaea* could be linked to an inhibition of the photosynthetic process at higher temperatures. *C. caespitosa* and *C. inornata* show an increase in $\delta^{13}C$ and $\delta^{18}O$ with increasing maximum temperature

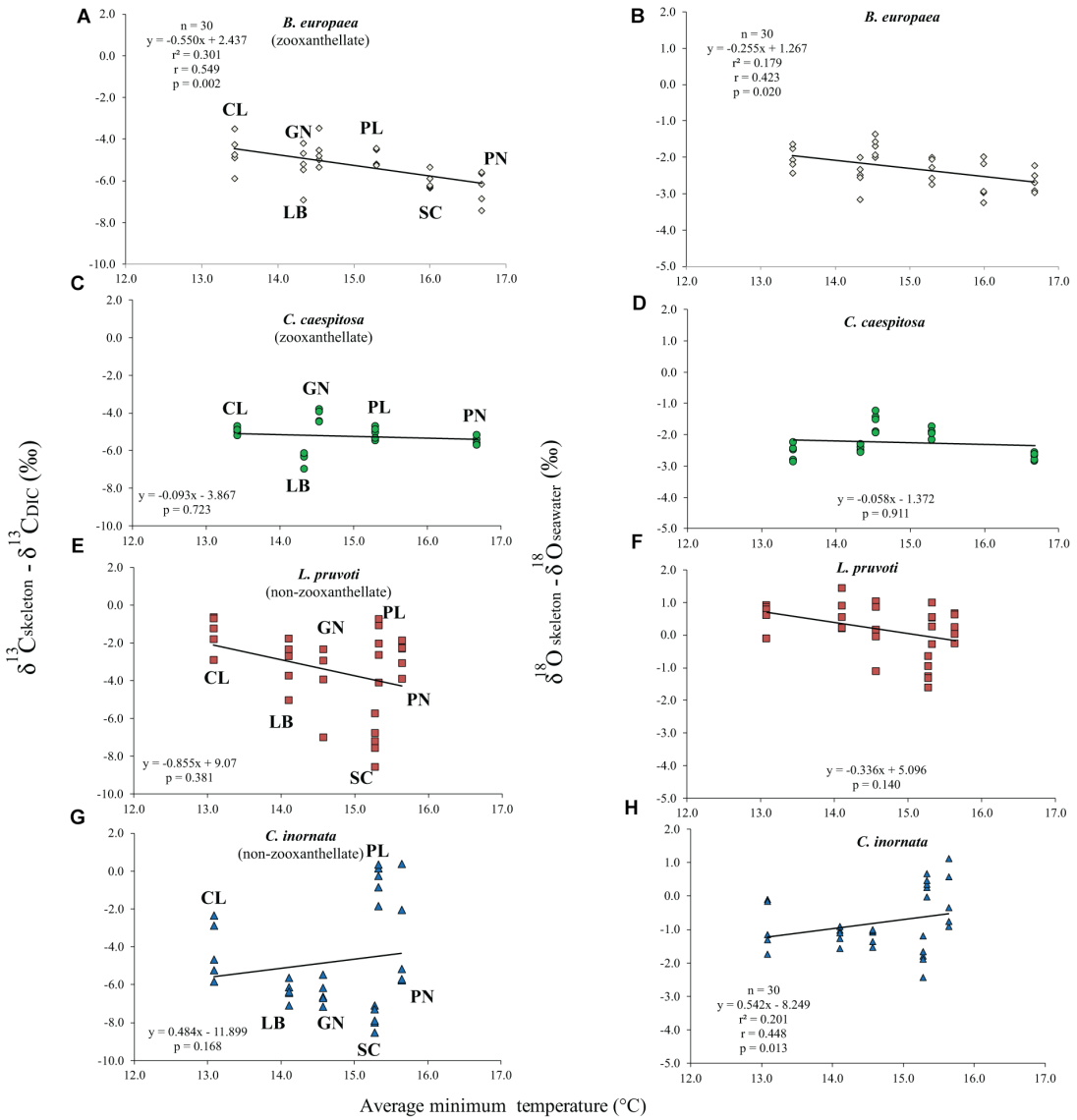

FIGURE 5 | The relation between skeletal $\delta^{13}C$ and $\delta^{18}O$ with average minimum temperature in *B. europaea* (temperature at 6 m; **A,B**), *C. caespitosa* (temperature at 6 m; **C,D**), *L. pruvoti* (temperature at 16 m; **E,F**), and *C. inornata* (temperature at 16 m; **G,H**). r^2, Spearman's determination coefficient; *r*, Spearman's correlation coefficient; *n*, number of individuals.

(**Figure 6**). A possible explanation for the pattern observed in *C. caespitosa* could be a reduction of the calcification with increasing temperature. Rodolfo-Metalpa et al. (2006) showed that long-term exposure to high temperature led to a decrease in net calcification of *C. caespitosa* (Rodolfo-Metalpa et al., 2006). However, further studies are needed on the growth of this species along the gradient to validate this hypothesis. Regarding the observed increase in $\delta^{13}C$ and $\delta^{18}O$ with increasing temperature we were not able to find any suitable explanation.

The discrimination between the "metabolic effects" and "kinetic isotope effects" is difficult. We adopt for this discussion McConnaughey's (1989a) definition that kinetic isotope effects are characterized by strong linear correlation between skeletal $\delta^{18}O$ and $\delta^{13}C$ due to discrimination against the heavy isotopes during CO_2 hydration and hydroxylation. Metabolic effects in McConnaughey's (1989a) involve additional positive or negative modulation of skeletal $\delta^{13}C$, reflecting changes in the $\delta^{13}C$ of DIC reservoir, caused mainly by photosynthesis and respiration. Our results show that the metabolic effect is not confined to affect carbon isotopes solely. The non-zooxanthellate *L. pruvoti* and *C. inornata* show twice the $\delta^{18}O$ disequilibrium range compared to the zooxanthellate corals *B. europaea* and *C. caespitosa* (**Figure 3**). This does not support the hypothesis that zooxanthellate and non-zooxanthellate corals attain about the same equilibrium value (McConnaughey, 1989a). The fact that zooxanthellate corals exhibit a narrower range

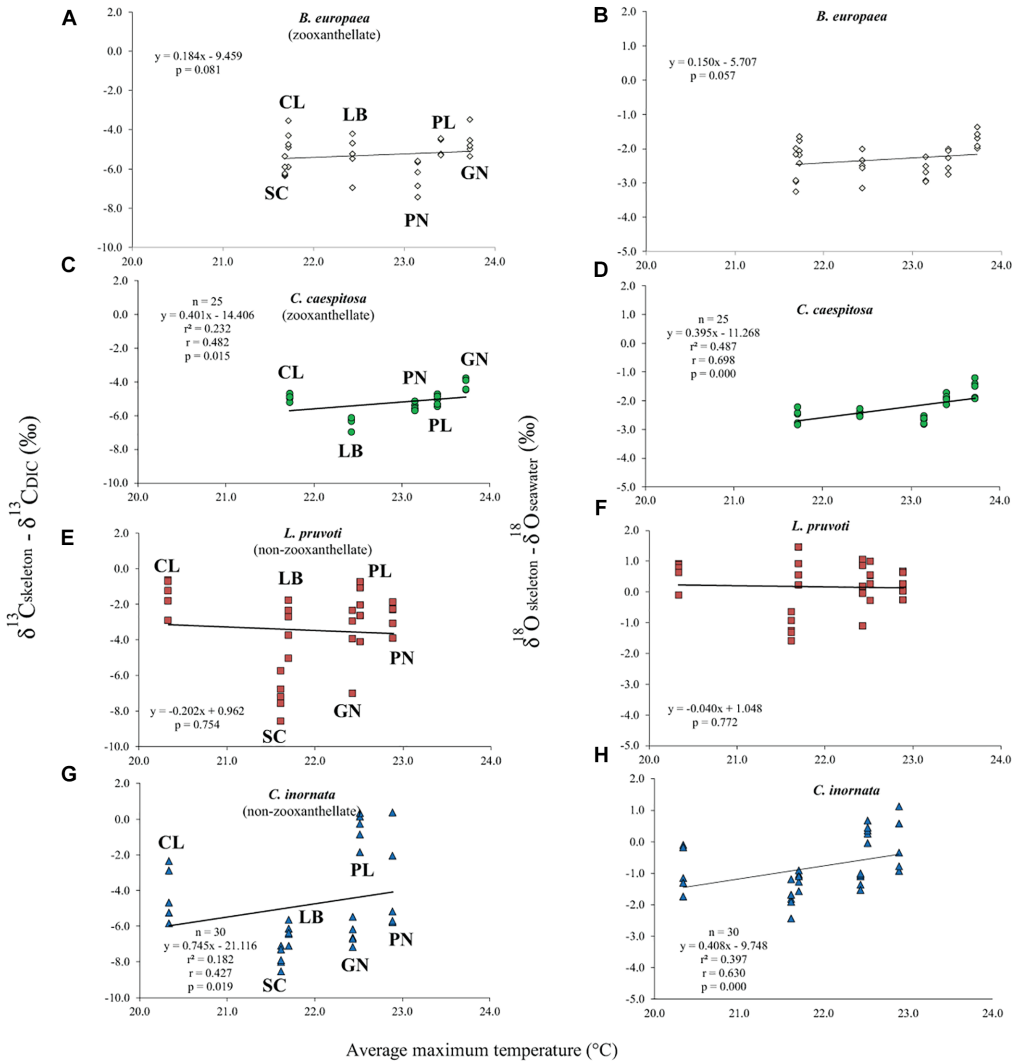

FIGURE 6 | The relation between skeletal $\delta^{13}C$ and $\delta^{18}O$ with average maximum temperature in *B. europaea* (temperature at 6 m; **A,B**), *C. caespitosa* (temperature at 6 m; **C,D**), *L. pruvoti* (temperature at 16 m; **E,F**), and *C. inornata* (temperature at 16 m; **G,H**). r^2, Spearman's determination coefficient; *r*, Spearman's correlation coefficient; *n*, number of individuals.

of skeletal $\delta^{18}O$ and $\delta^{13}C$, which are confined to the more depleted values, suggests that the photosynthetic activity restricts the corals to a narrow range of isotopic composition, away from isotopic equilibrium for both isotopes. In Adkins' model, which considers two major pools [CO_2 (aq)] and seawater DIC for the mineralization process, this indicates lower% seawater leak and/or higher pH at the calcifying fluid (Adkins et al., 2003). The wider range and the proximity of the skeletal isotope values to equilibrium values (**Figure 3**) observed in the non-zooxanthellate compared to the zooxanthellate corals investigated here suggest more seawater leak to the calcifying fluid and lower pH of calcification. This may seem apparently in disagreement with the higher ΔpH (pH of calcifying fluid minus pH of seawater) observed for deep-sea species compared to tropical and temperate aragonitic specie, which however, has been suggested as a mechanism to overcome the severe environmental limitations (low levels of carbonate saturation) of the deep ocean (McCulloch et al., 2012), which certainly do not apply to the shallow water non-zooxanthellate species considered here. Moreover, a larger contribution from ambient seawater to the calcifying fluid in non- zooxanthellate corals is supported by the observed higher porosity in *L. pruvoti* compared to *B. europaea* (Caroselli et al., 2011). The higher porosity may allow seawater to reach the calcification sites through vacuole transport through cells, channels between cells and gaps between calcifying tissues, and the skeleton (Furla et al., 1998). The Mediterranean shallow water zooxanthellate and non-zooxanthellate corals investigated in this study fit well the general relation between $\delta^{18}O$ and $\delta^{13}C$ of deep-sea species, including the observation of the "metabolic carbon offset," in the order of 1–2% (Adkins et al., 2003). However, the "Maximum membrane carbon flux" inflection point (i.e., at the most depleted carbon values $\delta^{13}C$

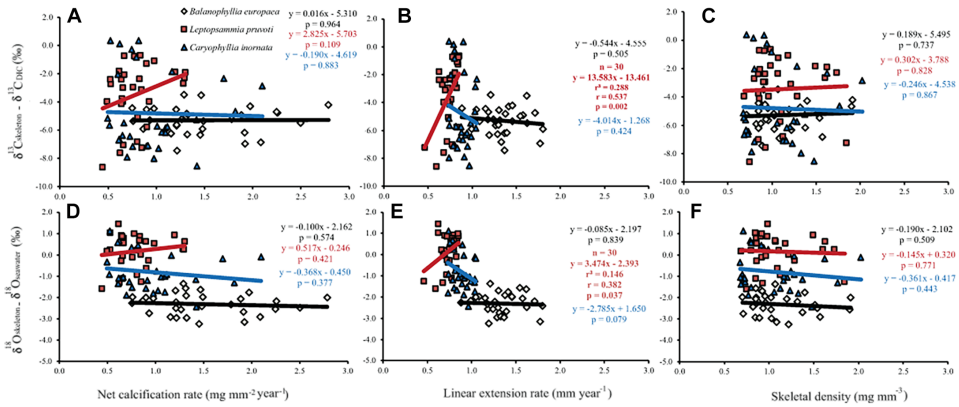

FIGURE 7 | The relation between skeletal $\delta^{13}C$ and $\delta^{18}O$ and net calcification rate (mg mm^{-2} yr^{-1}; **A,D**), linear extension rate (mm yr^{-1}; **B,E**) and skeletal bulk density (mg mm^{-3}; **C,F**) in *B. europaea*, *L. pruvoti*, and *C. inornata* at 6 sites along the west coast of Italy (~850 km transect). Net calcification rate, linear extension rate and skeletal density data were taken from Goffredo et al. (2009) and Caroselli et al. (2012a, 2016b). r^2, Pearson's coefficient of determination; *r*, Pearson's correlation coefficient; *n*, number of individuals.

remains constant while $\delta^{18}O$ continues to decrease), observed in deep-sea corals is not found in our data (Adkins et al., 2003).

For a given value of $\delta^{18}O$, the zooxanthellate Mediterranean species have heavier $\delta^{13}C$ compared to the non-zooxanthellate corals (**Figure 3**), in agreement with previous studies suggesting that photosynthesis enriches skeletal $\delta^{13}C$ (Swart, 1983; McConnaughey, 1989a). Only a limited number of individual non-zooxanthellate corals exhibit skeletal $\delta^{18}O$ equilibrium values while all $\delta^{13}C$ values in the four Mediterranean species are depleted in comparison to the estimated isotopic equilibrium with ambient seawater. This suggests that temperate corals cannot be used for thermometry-based seawater reconstruction. The weak temperature dependency of *B. europaea* with average minimum temperature might be the exception (**Figure 5**). Also, the strong kinetic effect suggested by the high correlation between $\delta^{18}O$ and $\delta^{13}C$ observed in the zooxanthellate species likely prevents the use of these species as proxies of cloud cover, seasonality, and nutrient/zooplankton levels (e.g., Grottoli and Wellington, 1999; Heikoop et al., 2000; Grottoli, 2002).

CONCLUSION

The skeletal stable isotopic signatures of individual specimens of zooxanthellate and non-zooxanthellate Mediterranean coral species collected along an 8° latitudinal gradient on the Western Italian coast were assessed. Considering the ~2°C (annual average SST) temperature difference and the homogeneity of the seawater $\delta^{18}O$ and $\delta^{13}C_{DIC}$ measured along the gradient, the wide variation in both skeletal $\delta^{18}O$ and $\delta^{13}C$ (~2 to ~4‰ and ~4 to ~9‰, respectively) among species may be attributed to metabolic/kinetic effects. In spite of the extensive effort to differentiate between the "carbonate" model and the "kinetic" model as controlling coral calcification (Adkins et al., 2003; McConnaughey, 2003; Chen et al., 2018), our data show that individual corals within the same species express the full range of isotope fractionation, suggesting strong metabolic contributions in addition to the kinetic isotope effect in these temperate corals. Therefore, we conclude that precipitation of coral skeletal aragonite likely occurs under controlled kinetic biological processes, rather than thermodynamic control alone, following a mechanism that is yet to be unraveled.

DATA AVAILABILITY

The raw data supporting the conclusions of this manuscript will be made available by the authors, without undue reservation, to any qualified researcher.

ETHICS STATEMENT

Being non-cephalopod invertebrates, the animals used in this study (Cnidaria, Scleractinia) are not included in the Directive 2010/63/EU of the European Parliament and of the Council of 22 September 2010 on the protection of animals used for scientific purposes. For this reason, no ethical statement is needed.

AUTHOR CONTRIBUTIONS

ZD, GF, and SG conceived and designed the research. FP, EC, and SG collected the specimens and provided the background data. RY, OL, and AS analyzed the samples. FP performed the statistical analyses. FP, RY, OL, SG, and AS participated in the scientific discussion. All authors contributed to the writing of the manuscript and gave final approval for publication.

FUNDING

The research leading to these results was supported by the European Research Council under the European Union's Seventh Framework Programme (FP7/2007-2013)/ERC grant agreement

number (249930- CoralWarm: Corals and global warming: the Mediterranean versus the Red Sea). EC was supported by the ALMA IDEA grant of the University of Bologna for the project "STRAMICRO."

ACKNOWLEDGMENTS

The authors would like to thank the diving centers Centro Immersioni Pantelleria, Il Pesciolino, Bubble Lounge, and Sub Maldive for their logistic assistance in the field. The Scientific Diving School (www.sdseducational.org) provided the technical and logistical support. The De Botton Center for Marine Science at the Weizmann Institute provided partial support.

SUPPLEMENTARY MATERIAL

The Supplementary Material for this article can be found online at: https://www.frontiersin.org/articles/10.3389/fmars.2019.00522/full#supplementary-material

REFERENCES

Adkins, J. F., Boyle, E. A., Curry, W. B., and Lutringer, A. (2003). Stable isotopes in deep-sea corals and a new mechanism for "vital effects". *Geochim. Cosmochim. Acta* 67, 1129–1143. doi: 10.1016/S0016-7037(02)01203-6

Airi, V., Gizzi, F., Falini, G., Levy, O., Dubinsky, Z., and Goffredo, S. (2014). Reproductive efficiency of a Mediterranean endemic *Zooxanthellate* coral decreases with increasing temperature along a wide latitudinal gradient. *PLoS One* 9:e91792. doi: 10.1371/journal.pone.0091792

Al-Horani, F. A. (2005). Effects of changing seawater temperature on photosynthesis and calcification in the scleractinian coral *Galaxea fascicularis*, measured with O2, Ca2+ and pH micro-sensors. *Sci. Mar.* 69, 347–354. doi: 10.3989/scimar.2005.69n3347

Al-Horani, F. A., Al-Moghrabi, S. M., and De Beer, D. (2003). The mechanism of calcification and its relation to photosynthesis and respiration in the scleractinian coral *Galaxea fascicularis*. *Mar. Biol.* 142, 419–426. doi: 10.1007/s00227-002-0981-8

Allemand, D., Ferrier-Pagès, C., Furla, P., Houlbrèque, F., Puverel, S., Reynaud, S., et al. (2004). Biomineralisation in reef-building corals: from molecular mechanisms to environmental control. *C. R. Palevol* 3, 453–467. doi: 10.1016/j.crpv.2004.07.011

Al-Rousan, S., Al-Moghrabi, S., Patzold, J., and Wefer, G. (2003). Stable oxygen isotopes in *Porites* corals monitor weekly temperature variations in the northern Gulf of Aqaba. *Red Sea. Coral Reefs* 22, 346–356. doi: 10.1007/s00338-003-0321-6

Altman, D. G. (1991). *Practical Statistics for Medical Research*. New York, NY: Chapman & Hall, CRC, 624.

Asami, R., Yamada, T., Iryu, Y., Meyer, C. P., Quinn, T. M., and Paulay, G. (2004). Carbon and oxygen isotopic composition of a Guam coral and their relationships to environmental variables in the western Pacific. *Paleogeogr. Paleoclimatol. Paleoecol.* 212, 1–22. doi: 10.1016/j.palaeo.2004.05.014

Böhm, F., Joachimski, M. M., Dullo, W. C., Eisenhauer, A., Lehnert, H., Reitner, J., et al. (2000). Oxygen isotope fractionation in marine aragonite of coralline sponges. *Geochim. Cosmochim. Acta* 64, 1695–1703. doi: 10.1016/S0016-7037(99)00408-1

Caroselli, E., Brambilla, V., Ricci, F., Mattioli, G., Levy, O., Falini, G., et al. (2016a). Inferred calcification rate of a temperate a*Zooxanthellate* caryophylliid coral along a wide latitudinal gradient. *Coral Reefs* 35, 919–928. doi: 10.1007/s00338-016-1422-3

Caroselli, E., Ricci, F., Brambilla, V., Mattioli, G., Levy, O., Falini, G., et al. (2016b). Relationships between growth, population dynamics, and environmental parameters in the solitary non-*Zooxanthellate* scleractinian coral *Caryophyllia inornata* along a latitudinal gradient in the Mediterranean Sea. *Coral Reefs* 35, 507–519. doi: 10.1007/s00338-015-1393-9

Caroselli, E., Falini, G., Goffredo, S., Dubinsky, Z., and Levy, O. (2015). Negative response of photosynthesis to natural and projected high seawater temperatures estimated by pulse amplitude modulation fluorometry in a temperate coral. *Front. Physiol.* 6:317. doi: 10.3389/fphys.2015.00317

Caroselli, E., Mattioli, G., Levy, O., Falini, G., Dubinsky, Z., and Goffredo, S. (2012a). Inferred calcification rate of a Mediterranean *aZooxanthellate* coral is uncoupled with sea surface temperature along an 8° latitudinal gradient. *Front. Zool.* 9:32. doi: 10.1186/1742-9994-9-32

Caroselli, E., Zaccanti, F., Mattioli, G., Falini, G., Levy, O., Dubinsky, Z., et al. (2012b). Growth and demography of the solitary scleractinian coral *Leptopsammia pruvoti* along a sea surface temperature gradient in the Mediterranean Sea. *PLoS One* 7:e37848. doi: 10.1371/journal.pone.0037848

Caroselli, E., Prada, F., Pasquini, L., Nonnis Marzano, F., Zaccanti, F., Falini, G., et al. (2011). Environmental implications of skeletal micro-density and porosity variation in two scleractinian corals. *Zoology* 114, 255–264. doi: 10.1016/j.zool.2011.04.003

Carricart-Ganivet, J. P. (2004). Sea surface temperature and the growth of the west Atlantic reef-building coral *Montastraea annularis*. *J. Exp. Mar. Biol. Ecol.* 302, 249–260. doi: 10.1016/j.jembe.2003.10.015

Chen, S., Gagnon, A. C., and Adkins, J. F. (2018). Carbonic anhydrase, coral calcification and a new model of stable isotope vital effects. *Geochim. Cosmochim. Acta.* 236, 179–197. doi: 10.1016/j.gca.2018.02.032

Cohen, A. L., Gaetani, G. A., Lundälv, T., Corliss, B. H., and George, R. Y. (2006). Compositional variability in a cold-water scleractinian, *Lophelia pertusa*: new insights into "vital effects". *Geochem. Geophys. Geosyst.* 7:Q12004. doi: 10.1029/2006GC001354

Cohen, A. L., Layne, G. D., Hart, S. R., and Lobel, P. S. (2001). Kinetic control of skeletal Sr/Ca in a symbiotic coral: implications for the paleotemperature proxy. *Paleoceanography* 16, 20–26. doi: 10.1029/1999PA000478

Cohen, A. L., and McConnaughey, T. A. (2003). Geochemical perspectives on coral mineralization. *Rev. Mineral Geochem.* 54, 151–187. doi: 10.2113/0540151

CorreÌge, T. (2006). Sea surface temperature and salinity reconstruction from coral geochemical tracers. *Palaeogeogr. Palaeoclimatol. Palaeoecol.* 232, 408–428. doi: 10.1016/j.palaeo.2005.10.014

Cortese, G., and De Domenico, E. (1990). Some considerations on the levantine intermediate water distribution in the Straits of Messina. *Boll. Ocean. Teor. Appl.* 8, 197–207.

Craig, H. (1961). Isotopic variations in meteoric waters. *Science* 133, 1702–1703. doi: 10.1126/science.133.3465.1702

Cullen, J. J., and Neale, P. J. (1994). Ultraviolet radiation, ozone depletion, and marine photosynthesis. *Photosyn. Res.* 39, 303–320. doi: 10.1007/BF00014589

D'Ortenzio, F., and Ribera d'Alcalà, M. (2009). On the trophic regimes of the Mediterranean sea: a satellite analysis. *Biogeosciences* 6, 139–148. doi: 10.5194/bg-6-139-2009

Epstein, S., Buchsbaum, R., Lowenstam, H. A., and Urey, H. C. (1951). Carbonate-water isotopic temperature scale. *Bull. Geol. Soc. Am.* 62, 417–426.

Epstein, S., Buchsbaum, R., Lowenstam, H. A., and Urey, H. C. (1953). Revised carbonate water isotopic temperature scale. *Bull. Geol. Soc. Am.* 64, 1315–1325.

Erez, J. (1978). Vital effect on stable-isotope composition seen in foraminifera and coral skeletons. *Nature* 273, 199–202. doi: 10.1038/273199a0

Fantazzini, P., Mengoli, S., Evangelisti, S., Pasquini, L., Mariani, M., Brizi, L., et al. (2013). A time-domain nuclear magnetic resonance study of Mediterranean scleractinian corals reveals skeletal-porosity sensitivity to environmental changes. *Environ. Sci. Technol.* 47, 12679–12686. doi: 10.1021/es402521b

Felis, T., Pätzold, J., and Loya, Y. (2003). Mean oxygen-isotope signatures in *Porites* spp. corals: inter-colony variability and correction for extension-rate effects. *Coral Reefs* 22, 328–336. doi: 10.1007/s00338-003-0324-3

Ferrier-Pagès, C., Reynaud, S., and Allemand, D. (2012). "Shallow water *scleractinian* corals of the Mediterranean Sea," in *Life in the Mediterranean Sea:*

a Look at Habitat Changes, ed. N. Stambler (Hauppauge, NY: Nova Sciences Publishers, Inc), 387–422.

Furla, P., Bénazet-Tambutté, S., Jaubert, J., and Allemand, D. (1998). Diffusional permeability of dissolved inorganic carbon through the isolated oral epithelial layers of the sea anemone, Anemonia viridis. *J. Exp. Mar. Biol. Ecol.* 221, 71–88. doi: 10.1016/S0022-0981(97)00116-0

Furla, P., Galgani, I., and Durand, I. (2000). Sources and mechanisms of inorganic carbon transport for coral calcification and photosynthesis. *J. Exp. Biol.* 203, 3445–3457.

Gabriel, K. R., and Lachenbruch, P. A. (1969). Non-parametric ANOVA in small samples: a monte carlo study of the adequacy of the asymptotic approximation. *Biometrics* 25, 593–596. doi: 10.2307/2528915

Gagan, M. K., Ayliffe, L. K., Beck, J. W., Cole, J. E., Druffel, E. R. M., Dunbar, R. B., et al. (2000). New views of tropical paleoclimates from corals. *Quat. Science Rev.* 19, 45–64. doi: 10.1016/S0277-3791(99)00054-2

Gat, J. R., Shemesh, A., Tziperman, E., Hecht, A., Georgopoulos, D., and Basturk, O. (1996). The stable isotope composition of waters of the eastern Mediterranean sea. *J. Geophys. Res.* 101, 6441–6451. doi: 10.1029/95jc02829

Gattuso, J.-P., Frankignoulle, M., and Smith, S. V. (1999). Measurement of community metabolism and significance in the coral reef CO_2 source-sink debate. *Proc. Natl. Acad. Sci. U.S.A.* 96, 13017–13022. doi: 10.1073/pnas.96.23.13017

Goffredo, S., Caroselli, E., Mattioli, G., Pignotti, E., Dubinsky, Z., and Zaccanti, F. (2009). Inferred level of calcification decreases along an increasing temperature gradient in a Mediterranean endemic coral. *Limnol. Oceanogr.* 54, 930–937. doi: 10.4319/lo.2009.54.3.0930

Goffredo, S., Caroselli, E., Mattioli, G., Pignotti, E., and Zaccanti, F. (2008). Relationships between growth, population structure and sea surface temperature in the temperate solitary coral *Balanophyllia europaea* (Scleractinia, Dendrophylliidae). *Coral Reefs* 27, 623–632. doi: 10.1007/s00338-008-0362-y

Goffredo, S., Caroselli, E., Pignotti, E., Mattioli, G., and Zaccanti, F. (2007). Variation in biometry and population density of solitary corals with environmental factors in the Mediterranean Sea. *Mar. Biol.* 152, 351–361. doi: 10.1007/s00227-007-0695-z

Goffredo, S., Mancuso, A., Caroselli, E., Prada, F., Dubinsky, Z., Falini, G., et al. (2015). Skeletal mechanical properties of Mediterranean corals along a wide latitudinal gradient. *Coral Reefs* 34, 121–132. doi: 10.1007/s00338-014-1222-6

Goreau, T. J. (1977a). "Carbon metabolism in calcifying and photosynthetic organisms: theoretical models based on stable isotope data," in *Proceedings of the 3rd International Coral Reef Symposium*, Vol. 2, (Miami), 395–401.

Goreau, T. J. (1977b). Coral skeletal chemistry: physiological and environmental regulation of stable isotopes and trace elements in *Montastrea annularis*. *Proc. Roy. Soc. Lond. B* 196, 291–315. doi: 10.1098/rspb.1977.0042

Grossman, E. L., and Ku, T.-L. (1986). Oxygen and carbon isotope fractionation in biogenic aragonite: temperature effects. *Chem. Geol.* 59, 59–74. doi: 10.1016/0168-9622(86)90057-6

Grottoli, A. G. (2002). Effect of light and brine shrimp levels on skeletal d13C values in the Hawaiian coral *Porites compressa*: a tank experiment. *Geochim. Cosmochim. Acta* 66, 1955–1967. doi: 10.1016/S0016-7037(01)00901-2

Grottoli, A. G., and Wellington, G. M. (1999). Effect of light and *zooplankton* on skeletal d13C values in the eastern pacific corals *Pavona clavus* and *Pavona gigantea*. *Coral Reefs* 18, 29–41. doi: 10.1007/s003380050150

Heikoop, J. M., Dunn, J. J., Risk, M. J., Schwarcz, H. P., McConnaughey, T. A., and Sandeman, I. M. (2000). Separation of kinetic and metabolic isotope effects in carbon-13 records preserved in reef coral skeletons. *Geochim. et Cosmochim. Acta* 64, 975–987. doi: 10.1016/S0016-7037(99)00363-4

Iluz, D., and Dubinsky, Z. (2015). Coral photobiology: new light on old views. *Zoology* 118, 71–78. doi: 10.1016/j.zool.2014.08.003

Juillet-Leclerc, A., Rollion-Bard, C., Reynaud, S., and Ferrier-Pagès, C. (2018). A new paradigm for δ18O in coral skeleton oxygen isotope fractionation response to biological kinetic effects. *Chem. Geol.* 483, 131–140. doi: 10.1016/j.chemgeo.2018.02.035

Kružiæ, P., Sršen, P., and Benkoviæ, L. (2012). The impact of seawater temperature on coral growth parameters of the colonial coral *Cladocora caespitosa* (Anthozoa, Scleractinia) in the eastern Adriatic sea. *Facies* 58, 477–491. doi: 10.1007/s10347-012-0306-4

Kuhnert, H., Pätzold, J., Wyrwoll, K. H., and Wefer, G. (2000). Monitoring climate variability over the past 116 years in coral oxygen isotopes from Ningaloo reef, Western Australia. *Int. J. Earth Sci.* 88, 725–732. doi: 10.1007/s005310050300

Land, L. S., Lang, J. C., and Barnes, D. J. (1975). Extension rate: a primary control on the isotopic composition of west Indian (Jamaican) scleractinian reef coral skeletons. *Mar. Biol.* 33, 221–233. doi: 10.1007/BF00390926

Levy, O., Rosenfeld, M., Yam, R., and Shemesh, A. (2006). Heterogeneity of coral skeletons isotopic compositions during the 1998 bleaching event. *Limnol. Oceanogr.* 51, 1142–1148. doi: 10.4319/lo.2006.51.2.1142

Linsley, B. K., Kaplan, A., Gouriou, Y., Salinger, J., deMenocal, P. B., Wellington, G. M., et al. (2006). Tracking the extent of the south pacific convergence zone since the early 1600s. *Geochem. Geophys. Geosyst.* 7:Q05003. doi: 10.1029/2005GC001115

López Correa, M., Montagna, P., Vendrell-Simón, B., McCulloch, M., and Taviani, M. (2010). Stable isotopes (δ18O and δ13C), trace and minor element compositions of recent scleractinians and last glacial bivalves at the santa maria di leuca deep-water coral province, Ionian Sea. *Deep Sea Res. Part II Top. Stud. Oceanogr.* 57, 471–486. doi: 10.1016/j.dsr2.2009.08.016

Lough, J. M., and Barnes, D. J. (2000). Environmental controls on growth of the massive coral *Porites*. *J. Exp. Mar. Biol. Ecol.* 245, 225–243. doi: 10.1016/S0022-0981(99)00168-9

McConnaughey, T. (1989a). 13C and 18O isotopic disequilibrium biological carbonates: I. *Patterns. Geochim. Cosmochim. Acta* 53, 151–162. doi: 10.1016/0016-7037(89)90282-2

McConnaughey, T. (1989b). 13C and 18O isotopic disequilibrium biological carbonates: II In vitro simulation of kinetic isotope effects. *Geochim. Cosmochim. Acta* 53, 163–171. doi: 10.1016/0016-7037(89)90283-4

McConnaughey, T. A. (2003). Sub-equilibrium oxygen-18 and carbon-13 levels in biological carbonates: carbonate and kinetic models. *Coral Reefs* 22, 316–327. doi: 10.1007/s00338-003-0325-2

McConnaughey, T. A., Burdett, J., Whelan, J. F., and Paull, C. K. (1997). Carbon isotopes in biological carbonates: Respiration and photosynthesis. *Geochim. Cosmochim. Acta.* 61, 611–622. doi: 10.1016/S0016-7037(96)00361-4

McCulloch, M., Trotter, J., Montagna, P., Falter, J., Dunbar, R., Freiwald, A., et al. (2012). Resilience of cold-water scleractinian corals to ocean acidification: boron isotopic systematics of pH and saturation state up-regulation. *Geochim. Cosmochim. Acta* 87, 21–34. doi: 10.1016/j.gca.2012.03.027

McCulloch, M. T., Tudhope, A. W., Esat, T. M., Mortimer, G. E., Chappell, J., Pillans, B., et al. (1999). Coral record of equatorial sea-surface temperatures during the penultimate deglaciation at Huon Peninsula. *Science* 283, 202–204. doi: 10.1126/science.283.5399.202

Meibom, A., Cuif, J., Hillion, F., Constantz, B. R., Juillet-Leclerc, A., Dauphin, Y., et al. (2004). Distribution of magnesium in coral skeleton. *Geophys. Res. Lett.* 31:L23306. doi: 10.1029/2004GL021313

Meibom, A., Mostefaoui, S., Cuif, J. P., Dauphin, Y., Houlbrèque, F., Dunbar, R., et al. (2007). Biological forcing controls the chemistry of reef-building coral skeleton. *Geophys. Res. Lett.* 34:L02601. doi: 10.1029/2006GL028657

Meibom, A., Stage, M., Wooden, J., Constantz, B. R., Dunbar, R. B., Owen, A., et al. (2003). Monthly Strontium/Calcium oscillations in symbiotic coral aragonite: biological effects limiting the precision of the paleotemperature proxy. *Geophys. Res. Lett.* 30:1418. doi: 10.1029/2002GL016864

Montagna, P., Silenzi, S., Devoti, S., Mazzoli, C., McCulloch, M., Scicchitano, G., et al. (2008). Climate reconstructions and monitoring in the Mediterranean sea: a review on some recently discovered high-resolution marine archives. *Rend. Lincei Sci. Fis. Nat.* 19, 121–140. doi: 10.1007/s12210-008-0007-7

Paul, H. A., Bernasconi, S. M., Schmid, D. W., and McKenzie, J. A. (2001). Oxygen isotopic composition of the Mediterranean sea since the last glacial maximum: constraints from pore water analyses. *Earth Planet. Sci. Lett.* 192, 1–14. doi: 10.1016/s0012-821x(01)00437-x

Peirano, A., Morri, C., and Bianchi, C. N. (1999). Skeleton growth and density pattern of the temperate, zooxanthellate scleractinian *Cladocora caespitosa* from the Ligurian sea (NW Mediterranean). *Mar. Ecol. Prog. Ser.* 185, 195–201. doi: 10.3354/meps185195

Peirano, A., Morri, C., Bianchi, C. N., Aguirre, J., Antonioli, F., Calzetta, G., et al. (2004). The Mediterranean coral *Cladocora caespitosa*: a proxy for past climate fluctuations? *Glob. Planet. Change* 40, 195–200. doi: 10.1016/S0921-8181(03)00110-3

Pierre, C., Vergnaud-Grazzini, C., Thouron, D., and Saliege, J. F. (1986). Compositions isotopiques de l'oxygène et du carbone des masses d'eau en Méditerranée. *Mem. Soc. Geol. Ital* 36, 165–174.

Potvin, C., and Roff, D. A. (1993). Distribution-free and robust statistical methods: viable alternatives to parametric statistics? *Ecology* 74, 1617–1628. doi: 10.2307/1939920

Rodolfo-Metalpa, R., Richard, C., Allemand, D., and Ferrier-Pagès, C. (2006). Growth and photosynthesis of two Mediterranean corals, *Cladocora caespitosa* and *Oculina patagonica*, under normal and elevated temperatures. *J. Exp. Biol.* 209, 4546–4556. doi: 10.1242/jeb.02550

Rodrigues, L. J., and Grottoli, A. G. (2006). Calcification rate and the stable carbon, oxygen, and nitrogen isotopes in the skeleton, host tissue, and *Zooxanthellae* of bleached and recovering Hawaiian corals. *Geochim. Cosmochim. Acta* 70, 2781–2789. doi: 10.1016/j.gca.2006.02.014

Rollion-Bard, C., Chaussidon, M., and France-Lanord, C. (2003). pH control on oxygen isotopic composition of symbiotic corals. *Earth Planet. Sci. Lett.* 215, 275–288. doi: 10.1016/S0012-821X(03)00391-1

Romanek, C. S., Grossman, E. L., and Morse, J. W. (1992). Carbon isotopic fractionation in synthetic aragonite and calcite: effects of temperature and precipitation rate. *Geochim. Cosmochim. Acta* 56, 419–430. doi: 10.1016/0016-7037(92)90142-6

Sakalli, A. (2017). Sea surface temperature change in the Mediterranean sea under climate change: a linear model for simulation of the sea surface temperature up to 2100. *Appl. Ecol. Environ. Res* 15, 707–716. doi: 10.15666/aeer/1501_707716

Schoepf, V., Levas, S. J., Rodrigues, L. J., McBride, M. O., Aschaffenburg, M. D., Matsui, Y., et al. (2014). Kinetic and metabolic isotope effects in coral skeletal carbon isotopes: a re-evaluation using experimental coral bleaching as a case study. *Geochim. et Cosmochim. Acta* 146, 164–178. doi: 10.1016/j.gca.2014.09.033

Senchaudhuri, P., Mehta, C. R., and Patel, N. R. (1995). Estimating exact p-values by the method of control variates, or Monte Carlo rescue. *J. Am. Stat. Assoc.* 90, 640–648. doi: 10.1080/01621459.1995.10476558

Silenzi, S., Bard, E., Montagna, P., and Antonioli, F. (2005). Isotopic and elemental records in a non-tropical coral (*Cladocora caespitosa*): discovery of a new high-resolution climate archive for the Mediterranean sea. *Glob. Planet. Change* 49, 94–120. doi: 10.1016/j.gloplacha.2005.05.005

Smith, J. E., Schwarcz, H. P., Risk, M. J., McConnaughey, T., and Keller, N. (2000). Paleotemperatures from deep-sea corals: overcoming 'vital effects'. *Palaios* 15, 25–32. doi: 10.1669/0883-1351(2000)015<0025:pfdsco>2.0.co;2

Sournia, A. (1973). La production primaire planctonique en Mediterranee: essai de mise a jour. *Bull. Et. Comm. Medit. Special Issue* 5, 128.

Sueltemeyer, D., and Rinast, K.-A. (1996). The CO2 permeability of the plasma membrane of *Chlamydomonas reinhardtii*: mass-spectrometric 18O-exchange measurements from 13 C18 O2 in suspensions of carbonic anhydrase-loaded plasma-membrane vesicles. *Planta* 200, 358–368.

Swart, P. K. (1983). Carbon and oxygen isotope fractionation in scleractinian corals: a review. *Earth Sci. Rev.* 19, 51–80. doi: 10.1016/0012-8252(83)90076-4

Trotter, J. A., Montagna, P., McCulloch, M. T., Silenzi, S., Reynaud, S., Mortimer, G., et al. (2011). Quantifying the pH 'vital effect' in the temperate *Zooxanthellate* coral *Cladocora caespitosa*: validation of the boron seawater pH proxy. *Earth Planet. Sci. Lett.* 303, 163–173. doi: 10.1016/j.epsl.2011.01.030

Urey, H. C., Lowenstam, H. A., Epstein, S., and McKinney, C. R. (1951). Measurement of paleotemperatures and temperatures of the upper cretaceous of England, Denmark, and the southeastern United States. *Bull. Geol. Soc. Am.* 62, 399–416.

Vidal-Dupiol, J., Zoccola, D., Tambutté, E., Grunau, C., Cosseau, C., Smith, K. M., et al. (2013). Genes related to ion-transport and energy production are upregulated in response to CO2-driven pH decrease in corals: new insights from transcriptome analysis. *PloS One* 8:e58652. doi: 10.1371/journal.pone.0058652

Vongsavat, V., Winotai, P., and Meejoo, S. (2006). Phase transitions of natural corals monitored by ESR spectroscopy. *Nucl. Instr. Meth. Phys. Res. B* 243, 167–173. doi: 10.1016/j.nimb.2005.07.197

Weber, J. M., Deines, P., Weber, P. H., and Baker, P. A. (1976). Depth-related changes in the 13C/12C ratio of coral carbonate deposited by the Caribbean reef-frame-building coral *Montastrea annularis*: further implications of a model for stable isotope fractionation by scleractinian corals. *Geochim. Cosmochim. Acta* 40, 31–39. doi: 10.1016/0016-7037(76)90191-5

Weber, J. N. (1974). 13C/12C ratios as natural isotopic tracers elucidating calcification processes in reef-building and non-reef-building corals. *Proc. Second. Intl. Coral Reef Symp.* 2, 289–298.

Weber, J. N., and Woodhead, P. M. (1972). Temperature dependence of oxygen-18 concentration in reef coral carbonates. *J. Geophys. Res.* 77, 463–473. doi: 10.1029/JC077i003p00463

Weber, J. N., and Woodhead, P. M. J. (1970). Carbon and oxygen isotope fractionation in the skeletal carbonate of reef-building corals. *Chem. Geol.* 6, 93–117. doi: 10.1016/0009-2541(70)90009-4

Wilbur, K. M., and Simkiss, K. (1979). Chapter 2.3 carbonate turnover and deposition by Metazoa. *Stud. Environ. Sci.* 3, 69–106. doi: 10.1016/S0166-1116(08)71055-0

Zoccola, D., Tambutteì, E., Kulhanek, E., Puverel, S., Scimeca, J.-C., Allemand, D., et al. (2004). Molecular cloning and localization of a PMCA P-type calcium ATPase from the coral *Stylophora pistillata*. *Biochim. Biophys. Acta* 1663, 117–126. doi: 10.1016/j.bbamem.2004.02.010

Conflict of Interest Statement: The authors declare that the research was conducted in the absence of any commercial or financial relationships that could be construed as a potential conflict of interest.